Supraspinal modulation of neuronal synchronization by nociceptive stimulation induces an enduring reorganization of dorsal horn neuronal connectivity

Contreras-Hernández E[1], Chávez D[1], Hernández E[1], Velázquez E[1], Reyes P[1], Bejar J[2], Martín M[2], Cortés U[2,3], Glusman S[1,4] and Rudomin P[1,5]

[1] Department of Physiology, Centro de Investigación y de Estudios Avanzados del Instituto Politécnico Nacional, México. [2]Universidad Politécnica de Catalunya. BarcelonaTech, Catalonia Spain, [3]Barcelona Supercomputing Center, Catalonia, Spain, [4]Stroger Cook County Hospital, USA, [5]El Colegio Nacional, México.

Short title: Supraspinal regulation of dorsal horn neuronal synchronization

Key Points

The state of central sensitization induced by the intradermic injection of capsaicin leads to structured (*non-random*) changes in functional connectivity between dorsal horn neuronal populations distributed along the spinal lumbar segments in anesthetized cats.

- The capsaicin-induced changes in neuronal connectivity and the concurrent increase in secondary hyperalgesia are transiently reverted by the systemic administration of small doses of lidocaine, a clinically effective procedure to treat neuropathic pain.
- The effects of both capsaicin and lidocaine are greatly attenuated in spinalized preparations, showing that supraspinal influences play a significant role in the shaping of nociceptive-induced changes in dorsal horn functional neuronal connectivity.
- We conclude that changes on functional connectivity between segmental populations of dorsal horn neurones induced by capsaicin and lidocaine result from a cooperative adaptive interaction between supraspinal and spinal neuronal networks, a process that may have a relevant role in the pathogenesis of chronic pain and analgesia.

Abstract

Despite the profuse information on the molecular and cellular mechanisms involved in the central sensitization produced by intense nociceptive stimulation, the changes in the patterns of functional connectivity between spinal neurones associated with the development of secondary hyperalgesia and allodynia remain largely unknown. Here we show that the state of central sensitization produced by the intradermal injection of capsaicin is associated with structured transformations in neuronal synchronization that lead to an enduring reorganization of the functional connectivity within a segmentally distributed ensemble of dorsal horn neurones. These changes are transiently reverted by the systemic administration of small doses of lidocaine, a clinically effective procedure to treat neuropathic pain. Lidocaine also reduces the capsaicin-induced facilitation of the spinal responses evoked by weak mechanical stimulation of the skin in the region of secondary but not in the region of primary hyperalgesia. The effects of both intradermic capsaicin and systemic lidocaine on the segmental correlation and coherence between ongoing cord dorsum potentials and on the responses evoked by tactile stimulation in the region of secondary hyperalgesia are greatly attenuated in spinalized preparations, showing that supraspinal influences are involved in the reorganization of the nociceptive-induced structured patterns of dorsal horn neuronal connectivity. We conclude that the structured reorganization of the functional connectivity between the dorsal horn neurones induced by capsaicin nociceptive stimulation results from cooperative interactions between supraspinal and spinal networks, a process that may have a relevant role in the shaping of the spinal state in the pathogenesis of chronic pain and analgesia.

Abbreviations: ANCOVA, covariance analysis; c, caudal; C1, cluster 1; C2, cluster 2; Cap, Capsaicin; CDPs, cord dorsum potentials; D-IFPs, deep intraspinal field potentials; IFPs, intraspinal field potentials; L, left; Lido, Lidocaine; Ps, slope p value; R, right; RMSS, root-mean square significance; r, rostral; S-IFPs, superficial intraspinal field potentials.

Introduction

Acute nerve damage or neuropathic and/or neurogenic inflammatory processes usually result in long lasting plastic changes in the nervous system such as central sensitization and reorganization of nociceptive pathways (Woolf 1983; Cook *et al*., 1987; Kaas, 1991; Wall *et al*., 2002). The process of spinal sensitization is an important component of the pain experience. It includes an enhancement of the functional status of neurones and circuits in nociceptive pathways that result in a state of facilitation, potentiation or amplification, leading to the perception of ongoing pain, hyperalgesia and allodynia (Woolf 2007; Latremoliere & Woolf, 2009; Basbaum *et al.,* 2009).

Studies in animal models have indicated that the inflammatory nociception induced by intradermic application of capsaicin leads to a prolonged state of central sensitization involving a fast reorganization of the cutaneous receptive fields of neurones in the cuneate nucleus (Pettit & Schwark, 1996). In anesthetized rats, capsaicin injected in the perioral region was also found to increase the ongoing firing of thalamo-cortical neurones and rapidly reorganize the whisker neuronal representations in both the thalamus and cortex (Katz *et al*., 1999). Other studies have revealed that these changes are also associated with alterations in the functional connectivity between dorsal horn neurones in the spinal cord. Thus, according to Eblen-Zajjur & Sandkühler (1996), most pairs of laminae III-V neurones with overlapping receptive fields showed increased correlated discharges during nociceptive stimulation and it has been suggested that these changes represent a stimulus-induced plasticity involving alterations in the strength and/or time of neuronal synchronization and rarely activation of new connections (see also Schaible *et al*., 1987; Biella *et al*., 1997; Galhardo *et al*., 2000;).

At peripheral level, the activation of C fibres by painful stimuli leads not only to the sensitization but also to long term potentiation at their central synapses referred to as secondary hyperalgesia that is reversed by brief application of a high opioid dose (Sandkuhler 2007, 2009; Sotgiu *et al*., 2009). Since this procedure also

92 reverses hyperalgesia in behaving animals, it has been suggested that opioids not
93 only temporarily dampen pain, but may also erase a spinal memory trace of pain
94 (Drdla-Schutting *et al*., 2012). Mechanical hyperalgesia may be associated with a
95 phenomenon similar to memory reconsolidation, a process by which memories are
96 rendered labile after reactivation and became susceptible to erasure (Bonin & De
97 Koninck, 2014).

98 Despite the increasing information on the cellular and molecular mechanisms
99 involved in the long lasting effects of acute nociceptive stimulation, there is limited
100 information pertaining the concurrent modifications of the patterns of functional
101 connectivity between dorsal horn neurones. Most studies have been addressed to
102 the analysis of the changes in synchronization between pairs of neurones usually
103 located within the same spinal segment (see Eblen-Zajjur & Sandkühler, 1996;
104 Biella *et al*., 1997; Galhardo *et al*., 2002; Roza *et al*., 2016) and few have
105 examined the reorganization of the functional connectivity between dorsal horn
106 neuronal populations located in different spinal segments, particularly during
107 nociceptive stimulation associated with the development of central sensitization
108 and its modulation by supraspinal influences (see Chávez *et al*., 2012; Chen *et al*.,
109 2015; Martin *et al*., 2015).

110 Previous studies in our laboratory have shown that the ongoing cord dorsum
111 potentials (CDPs) recorded in the lumbosacral segments of the anesthetized cat
112 are generated by the synchronous activity of a longitudinally distributed network of
113 interconnected local and intersegmental sets of dorsal horn neurones (Manjarrez *et*
114 *al.,* 2000, 2003 and Chávez *et al*., 2012). A key finding was that depending on the
115 level of neuronal synchronization, this ensemble could acquire specific
116 configurations of neuronal connectivity, some leading to the preferential activation
117 of the pathways mediating Ib non-reciprocal postsynaptic inhibition and others to
118 the activation of the pathways mediating primary afferent depolarization and
119 presynaptic inhibition (Contreras-Hernández *et al.,* 2015).

120 Based on these observations we assumed that the analysis of the changes
121 produced by nociceptive stimulation on the correlation and coherence between the

ongoing CDPs and intraspinal field potentials (IFPs) would be an appropriate mean to reveal relevant features of the supraspinal modulation of the patterns of functional connectivity between populations of dorsal horn neurones in different spinal segments associated with the development of both secondary hyperalgesia and allodynia, and to provide some insight on the mechanisms of action of clinically effective analgesic procedures (Mao & Chen, 2000; Fields, 2004; Challapalli *et al*., 2005; Endo *et al*., 2008; Sotgiu *et al*., 2009).

The present study was undertaken to examine in the anesthetized cat a) the effects of nociceptive neurogenic inflammatory input induced by the acute intradermic injection of capsaicin on the segmental distribution of correlation and coherence between the populations of dorsal horn neurones involved in the generation of the ongoing CDPs and IFPs, b) the extent to which these effects were modified by procedures clinically effective in the treatment of neuropathic pain such as the systemic injection of small clinically effective doses of lidocaine (Dirks *et al*., 2000; Tremont-Lukats, *et al*., 2006; Gordon & Schroeder, 2008) and c) the contribution of supraspinal influences on the capsaicin and lidocaine-induced effects on the functional connectivity between dorsal horn neurones and the possible relation of these changes with the development of mechanical allodynia and secondary hyperalgesia (see Urban & Gebhart, 1999; Abaei *et al*., 2016).

Some of these observations have been published in abstract form (Rudomin *et al*., 2012; Contreras-Hernández *et al*., 2013).

Materials and Methods

Ethical Approval

Cats were bred and housed under veterinarian supervision at the Institutional Animal Care unit (SAGARPA permission AUT-B-C-0114-007). They were kept in individual comfortable cages and had access to food and water *ad libitum.* All experiments were approved by the Institutional Ethics Committee for Animal Research (Protocol no. 126-03) and comply with the ethical policies and regulations of The Journal of Physiology, including the animal ethics checklist (see

Grundy, 2015). The Guide for Care and Use of Laboratory Animals (National Research Council, 2010) was followed in all cases.

General procedures

Preparation: The experiments were performed in 9 adult cats of either sex weighting between 2.5 and 3.5 Kg. The animals were initially anesthetized with pentobarbitone sodium (40 mg/kg i.p.). The carotid artery, radial vein, trachea and urinary bladder were cannulated. Additional doses of pentobarbitone sodium (5 mg/kg/hr) were given intravenously to maintain an adequate level of anesthesia, tested by assessing that withdrawal reflexes were absent, that the pupils were constricted and that systolic arterial blood pressure was between 100 and 120 mm Hg.

The lumbo-sacral and low thoracic spinal segments were exposed by laminectomy and opening of the dura mater. After the main surgical procedures, the animals were transferred to a stereotaxic metal frame allowing immobilization of the head and spinal cord and pools were made with the skin flaps that were filled with paraffin oil to prevent desiccation of the exposed tissues. The temperature was maintained between 36 and 37°C by means of radiant heat.

Subsequently, the animals were paralyzed with pancuronium bromide (0.1 mg/kg) and artificially ventilated. The tidal volume was adjusted to maintain 4% of CO_2 concentration in the expired air. During paralysis, adequacy of anaesthesia was ensured with supplementary doses of anesthetic (2 mg/kg in an hour) and by repeatedly assessing that the pupils remained constricted and that heart rate and blood pressure were not changed following a noxious stimulus (paw pinch). *Recording and stimulation:* CDPs were recorded by means of 8-12 silver ball electrodes placed on the surface of the L4-L7 segments on both sides of the spinal cord. To reduce cross-talk contributed by the indifferent electrode, differential recordings were made between the potentials recorded at each site against an equal number of electrodes, each inserted in the adjacent paravertebral muscles (see Malliani *et al*., 1965; Chávez *et al*., 2012; Obien *et al*., 2015).

In several experiments, in addition to the CDPs, we recorded the intraspinal field potentials (IFPs) with a pair of glass micropipettes filled with 2M NaCl (1-2 MΩ) that were inserted in the left side of the L6 segment with a rostro-caudal separation of 1 mm and positioned at two different depths within the dorsal horn, one superficial (500-800 µm) and another deeper (1600-1800 µm). Their final position was verified histologically (see below). Ongoing and evoked CDPs and IFPs were recorded with separate preamplifiers (band pass filters 0.3 Hz to 1 KHz), visualized on-line and digitally stored for further analysis with software written in MatLab (MathWorks) and LabView version 14 (National Instruments).

Spinalization: When effects of a spinal section were investigated, one of the exposed thoracic segments (usually T4-T6) was bathed with chilled ringer for about 10 minutes, sprayed with liquid nitrogen until it was completely frozen and sectioned to ensure complete and permanent interruption of supraspinal influences.

Mechanical stimulation of the skin: In several experiments we recorded the CDPs produced by mechanical stimulation of the skin by means of an air puff delivered by a Picospritzer (Intracel LTD) through two glass tubes (1 mm diameter) placed close to but without touching the skin on the left hindlimb. One of the tubes was placed near the site of capsaicin injection into the footpad and the other 35-40 mm centrally in the region of secondary hyperalgesia. The air puffs generated by the Picospritzer with pulses lasting 5-10 ms produced a change in pressure equivalent to 1g exerted by a von Frey hair leading to a tactile non-painful sensation when tested on ourselves.

Intradermic injection of capsaicin: As described by Rudomin & Hernández (2008), 30 µl of 1% solution of capsaicin diluted in 10% Tween 80 and 90% saline, (around 7.5 µg/kg) were injected in the plantar cushion of the left hindlimb. To avoid desensitization, capsaicin was injected only once (Sakurada *et al.*, 1992). In our experience the effects of capsaicin started around 10-20 min and attained maximum values between 100 and 180 min after the injection and persisted up to 4

hours. The injection of capsaicin produced a clear inflammatory response around the injection site (see Rudomin and Hernández, 2008).

Systemic injection of lidocaine: Lidocaine is a local anesthetic with short half-life (about 17 minutes) when systemically administered. In this series of experiments a solution of Lidocaine (5 mg/kg diluted in 6 cc of isotonic saline) was slowly injected (20-30 min) through a catheter inserted in the right femoral vein. An equivalent dose of systemic lidocaine has been used to treat neuropathic pain and to supplement general anesthesia (see Wallace *et al*., 1997; Gordon & Schroeder, 2008;).

Histology: At the end of the experiment the animal was euthanized with a pentobarbital overdose and perfused with 10% formalin. The spinal cord was removed for fixation and dehydration leaving the recording micropipettes in place. Subsequently, the spinal segments containing the micropipettes were placed in a solution of methyl salicylate for clearing and subsequently cut transversally to verify the position of the micropipettes. The tracks of the microelectrodes were drawn with a lucid camera (Wall & Werman, 1976).

Data processing

Coefficients of correlation: As in previous work (Chávez *et al*., 2012), the changes in correlation between the CDPs simultaneously recorded from different lumbo-sacral spinal segments were estimated by means of the Pearson correlation coefficient (ρ), as follows

$$Corr(X,Y) = \frac{\sum_{i=1}^{n}(x_i - \bar{x})(y_i - \bar{y})}{\sqrt{\sum_{i=1}^{n}(x_i - \bar{x})^2 \sum_{i=1}^{n}(y_i - \bar{y})^2}}$$

where X={xi} and Y={yi} are two voltage-time series corresponding to the continuous records of paired sets of CDPs and/or IFPs (lasting 5-10 min).

Power spectra and Coherence Function: To analyze the changes in the frequency components of the CDPs and of the IFPs we calculated the power spectra of the potentials recorded in individual spinal segments as well as the

frequency-dependence correlation (coherence function) between different paired sets of potentials.

The coherence function (γ) was calculated using the equations provided by the LabView v 14 tool kit as follows:

$$\gamma^2(\mathrm{f}) = \frac{\left(\text{Magnitude of the Average } S_{AB}(\mathrm{f})\right)^2}{\left(\text{Average } S_{AA}(\mathrm{f})\right)\left(\text{Average } S_{BB}(\mathrm{f})\right)}$$

where S_{AB} is the cross power spectrum, S_{AA} is the power spectrum of A, and S_{BB} is the power spectrum of B. This equation yields a coherence factor with a value between zero and one versus frequency.

Analysis of covariance (ANCOVA): This analysis was implemented in R software (R development, Core team, 2016) and used in some cases to compare changes in the slope (Ps) of the best linear fits of the correlation coefficients between paired sets of CDPs generated in the L4-L7 spinal segments. Ps values below 0.05 were considered as significant (see McDonald, 2014).

Randomness test: The randomness of each of the correlograms obtained during the different experimental conditions (Control, Capsaicin, Lidocaine and Spinalization) was examined by using the standard runs-test for randomness (Gibbons, 1996). Briefly, for a given correlogram we calculated the difference between each of the correlation values relative to the median value of the correlogram in order to obtain a sequence of binary relations (bigger than, less than). Same values were discarded. This test assumes sequentially ordered values. The binary relationship sequence patterns were analyzed to explore if they occurred by chance in a random arrangement (null hypothesis) by considering the number of runs-distribution. P-values below 0.05 were considered as significant.

We found that in the present set of experiments all correlograms showed a non-random significance below 0.005. This implies that the segmental patterns of correlation between ongoing CDPs during the control state as well as during the different experimental conditions are the expression of non-random states of

functional connectivity between the neuronal ensembles involved in the generation of the CDPs.

Similitude tests: Tests of similarity between the histograms of the coefficients of correlation obtained from the whole set of all the combinations of the paired sets of CDPs or IFPs obtained from 5-10 min recordings (correlograms) were made to compare the effects exerted by the different experimental procedures. To this end we calculated the root mean-square significance (RMSS) between pairs of correlograms. Briefly, given two correlograms X={x_i} and Y={y_i}, where x_i and $y_i$are the values on the i-th bin, corresponding to the correlation value between all the combinations of paired sets of CDPs. Significance between pairs of bins is defined as: $S_i = \frac{\hat{x}_i - \widehat{ky}_i}{\sqrt{\widehat{\sigma^2}_{xi} + \widehat{k\sigma^2}_{yi}}}$, where $k = {}^{N1}/_{N2}$, $\hat{x}_i$, $\widehat{\sigma^2}_{xi}$ and $\hat{y}_i$, $\widehat{\sigma^2}_{yi}$ are the expected and variance values of the i-ith bin and $N1$, $N2$ are the volumes of the correlograms (i.e. the sum of all their elements).

The RMSS values are calculated as follows: $RMSS = \sqrt{\frac{\sum_{i=1}^{M}(S_i - \hat{S})^2}{M}}$

where $\hat{S}$ is the mean value of S_i. RMSS≈0 indicates the same correlograms, RMSS≈1 indicates that the correlograms are different, but they come from the same parent population and RMSS>>1 indicates that correlograms are completely different.

The advantage of this test respect other tests is that allows the analysis of gradual changes in the shape of the correlograms produced by different procedures along the same experiment instead of forcing edge threshold levels to assess similitude. We consider this feature as an advantage because in our experience, changes induced by capsaicin or lidocaine develop gradually and rather slowly. See Bityukov *et al*., (2013) for further details.

Results

Systemic lidocaine transiently reverses the action of capsaicin on the correlation between ongoing CDPs and IFPs.

These observations were undertaken to examine the effects of the intradermic injection of capsaicin on the segmental correlation between the ongoing CDPs as well as of the correlation of the IFPs with the CDPs and their modification by the systemic administration of lidocaine and spinalization.

Fig. 1A-F shows the effects of the injection of capsaicin into the left plantar paw, of the systemic administration of lidocaine and of spinalization on the ongoing potentials recorded in the left and right sides of the L5 and L6 segments with 4 out of the 12 ball electrodes placed on the cord dorsum, as well as on the intraspinal field potentials recorded in the superficial (S-IFPs) and deeper layers (D-IFPs) with two micropipettes introduced in the left side of the L6 segment (see insert in Fig. 1A).

It may be seen that by one hour after the injection of capsaicin, the CDPs as well as the IFPs showed in addition to the relative brief potentials some slow synchronized activity (Fig. 1B). The injection of lidocaine (5 mg/kg administered systemically over 30 min) transiently reduced the slow synchronized potentials leaving brief CDPs and IFPs that resembled those recorded before the injection of capsaicin (Fig. 1C). Thereafter, when most of the lidocaine effects were over, the slow synchronized activity was resumed (Fig. 1D), suggesting a long lasting central effect induced by capsaicin (see Rudomin & Hernández 2008).

At this stage, a high spinalization (T4) removed the slow synchronized potentials and increased the frequency of the brief CDPs and IFPs (Fig. 1E). After spinalization, a second injection of lidocaine had minor effects on these potentials (Fig. 1F; see below).

Fig. 1G displays the time course of the changes produced by capsaicin, lidocaine and spinalization on the segmental correlation between the different combinations of paired sets of CDPs recorded with the whole set of 12 electrodes (66 in this case). The coefficients of correlation between the paired sets of CDPs obtained from a 10 min control recording period (Control 0) were arranged in descending order, displayed vertically and colored according to their magnitude (see scale). The coefficients obtained from subsequent 10 min non-overlapping

recordings were displayed *keeping the same order* that of the Control 0 coefficients. It may be seen that after the intradermic injection of capsaicin, the correlation between the paired sets of CDPs was briefly reduced and then began to increase and became rather high by 70-90 min. At this time the injected footpad was clearly inflamed (see Rudomin & Hernández, 2008).

The systemic injection of lidocaine (Lidocaine 1 in Fig. 1G) transiently reduced the capsaicin-induced increase in correlation between the CDPs. This effect was already detectable during the first 10 min after lidocaine administration and became largest 20 to 30 min later. By 40-50 min after lidocaine, the correlation between the CDPs increased again and went above the pre-lidocaine levels. At that time, spinalization at T4 abruptly reduced the correlation between the ongoing CDPs that was further reduced, albeit slightly, by a second injection of lidocaine (Lidocaine 2).

Similar changes have been observed on the correlation of the S-IFPs and D-IFPs with the CDPs (Figure 1H-I). It thus seems that the changes in correlation between paired sets of CDPs reflect the changes in correlation between the spinal neuronal networks detected by the intraspinal recordings (see below).

Segmental distribution of the changes in correlation

Correlation between paired sets of CDPs: We have assumed previously that the magnitude of the coefficients of correlation displayed by the paired sets of CDPs recorded from different segments reflects the strength of the functional connectivity between the neuronal ensembles receiving inputs from different parts of the hindlimb (Chávez *et al*., 2012).

To disclose the spatial (segmental) changes induced by capsaicin, lidocaine and spinalization on the correlation between the CDPs, the coefficients obtained from all the combinations of the paired sets of CDPs during a 10 min control recording period (Control 0) were plotted as horizontal bars, displayed in descending order (correlograms) and separated in 5 ranges according to their magnitude, each with a different color (see Fig. 2A). Thereafter, the segmental

location of the paired sets of CDPs *in each range* was indicated in a spinal cord diagram with the corresponding colored lines joining the recording sites (Fig. 2 A1-A4).

It may be seen in Fig. 2A1 that the highest control coefficients of correlation were displayed by paired sets of CDPs recorded from adjacent sites (black lines), while the coefficients in lower ranges (red to green lines) were displayed by paired sets of CDPs located in more distant segments in the same and in opposite sides of the spinal cord (Fig. 2 A2-A4). This distribution is consistent with the proposal of a longitudinally bilaterally distributed set of interconnected neuronal populations (Chávez *et al*., 2012; Contreras-Hernández *et al*., 2015).

Quite interestingly, 70-80 min after the injection of capsaicin there was a significant increase in the correlation between the crossed CDPs generated in nearby segments (Fig. 2B1) and a concurrent reduction in the correlation between the more distant sets of CDPs (Fig. 2 B2 and B3). 10-20 min after the systemic injection of lidocaine, the effect of capsaicin on the correlation between the CDPs was reversed (Fig. 2 C1 C4), and their segmental distribution resembled the control distribution as assessed by their relatively low RMSS (0.31).

The effect of lidocaine was over by 80-90 min after the injection (Fig. 2 D1-D4) and the spatial distribution of the correlation between the CDPs again resembled that induced by capsaicin before the administration of this local anesthetic (RMSS= 0.39). Spinalization also reduced the correlation, particularly that displayed by the crossed sets of CDPs (Fig. 2 E1-E4). The subsequent injection of lidocaine (20-30 min) had a small effect on the magnitude (RMSS=0.29) and segmental distribution of the correlation (Fig. 2 F1-F4).

Correlation between IFPs and CDPs: We expanded our observations on the correlated activity between the paired sets of CDPs to study the concurrent changes induced by capsaicin, lidocaine and spinalization on the correlation between the superficial and deep IFPs and the CDPs.

Under control conditions (Fig. 3A) the S-IFPs showed a weak correlation with the CDPs that was highest in segment L6cL. In contrast, as shown in Fig. 3G, the D-IFPs not only showed a higher correlation with the CDPs generated in L6cL (site of electrode insertion) but were also correlated with the CDPs generated in neighboring segments, including those in the opposite (right) side.

As described for the CDPs, 70-80 min after the injection of capsaicin the correlation between both IFPs and CDPs was also increased in both sides of the spinal cord. It was particularly stronger between the D-IFPs (recorded in laminae III-V) and the CDPs (Fig. 3B and H). A similar early (10 min) and late (80-90 min) effect of lidocaine occurred on the correlation patterns between the S-IFPs and the D-IFPs with the CDPs (Fig. 3C,D and Fig. 3I,J). They now resembled the control and capsaicin-induced patterns, respectively (see the RMSS values in figure).

Spinalization reduced the correlation between the IFPs and CDPs, but was still larger between the D-IFPs and the CDPs recorded in the left side (Fig. 3E and K). The effects on the correlation obtained 20-30 min after a second injection of lidocaine were rather small (RMSS= 0.23 and 0.27; Fig. 3F, L).

Altogether the above set of observations indicates that the effects of capsaicin and lidocaine on the correlation between the ongoing CDPs and between them and the IFPs are exerted not only on the temporal but also on the spatial (segmental) domain and that supraspinal influences contribute to the generation and modulation of the observed patterns of segmental connectivity between the populations of dorsal horn neurones in both sides of the spinal cord.

Differential action of capsaicin on the neuronal ensembles generating the CDPs

When plotting the control coefficients against the correlation coefficients obtained under different experimental procedures a different kind of information emerged that was not evident by just observing the changes in the correlograms.

Fig. 4A shows that the coefficients of correlation between the paired sets of CDPs obtained 0-10 min after the injection of capsaicin were still similar to the control 0 coefficients. However, by 40-50 min (Fig. 4B), these coefficients became separated in two distinct clusters and remained so for 20 min more (Fig. 4C), suggesting a *relatively stable* configuration of neuronal connectivity as assessed by the RMSS of 0.20 and the ANCOVA Ps values.

The two cluster arrangement induced by capsaicin was temporarily reverted by the systemic administration of lidocaine giving rise to a single cluster that remained practically unchanged for half an hour (RMSS=0.15 and Ps>0.05; Fig. 4D and E). Again, as the effect of lidocaine faded, the coefficients of correlation became assembled in two separate clusters that remained stable during half an hour (RMSS=0.30 and Ps >0.05; Fig. 4F and G). After spinalization they merged into a single cluster (Fig. 4H). A second injection of lidocaine reduced, albeit slightly, the correlation between the CDPs that still remained grouped into a single cluster (RMSS= 0.29; Fig. 4I).

Quite interestingly, we found that capsaicin also separated in two clusters the coefficients of correlation between the IFPs and the CDPs, that were reverted to a single cluster after lidocaine, as well as after spinalization performed once the action of lidocaine was over (Fig. 4J-R).

The two cluster arrangement induced by capsaicin was a rather unexpected finding and led to the question on its possible functional meaning. It clearly suggests a differential action on the neuronal ensembles involved in the generation of the CDPs and IFPs. To this end it seemed important to determine, in the first place, if there were any differences in the segmental location of the paired sets of potentials included in each of the two clusters. In this regard the data depicted in Fig. 3A-D provide part of the required information. They show that the major increase in correlation was displayed by the S-IFPs and D-IFPs versus the CDPs recorded in the caudal region of the L6 and rostral region of the L7 segments in both sides (L6cL, L6cR, L7rL, L7rR). These coefficients of correlation would contribute to the C2 cluster, Fig. 4C. The coefficients of correlation of the S-IFPs

and D-IFPs with the CDPs generated in the other, more distant segments (L6rL, L6rR, L5cL L5rL) would contribute to the C1 cluster. It should be noted that the L6cL and L7rL segments receive most of the nociceptive inputs generated by the injection of capsaicin (see Rudomin and Hernández 2008). Additional features of the capsaicin-induced separation of the coefficients of correlation in two clusters and their reversal by lidocaine are examined in the Discussion.

Consistency of effects of capsaicin and lidocaine in other preparations.

The data depicted in Figs. 1-4 were obtained from the same experiment. It thus seemed necessary to examine the effects of capsaicin and lidocaine on the segmental correlation between paired sets of CDPs in other preparations with intact neuroaxis. Fig. 5 summarizes the changes in correlation produced by capsaicin and lidocaine observed in other 3 experiments and Fig. 11 provides data from another experiment. As expected, the control correlograms were different in each experiment probably because of differences in the initial state of the preparation (e.g., anesthetic level). Yet, the overall effects of capsaicin and lidocaine were similar to those observed in the experiment of Figures 1-4. Namely, the intradermal injection of capsaicin produced a structured increase in the correlation between the paired sets of CDPs and this effect was transiently reversed following the systemic injection of lidocaine. The changes in the correlograms produced by the different procedures were validated with the similarity tests described above (see Figures).

In the experiment of Fig. 5A, we asked the question on the extent to which lidocaine would be able to revert the effects of capsaicin injected several hours before, at a time when according to Bonin and De Koninck (2014) there would be already a memory consolidation of the effects produced by the nociceptive stimulus. We found that the capsaicin-induced increase in correlation persisted for at least 4 hours and that at that time the systemic injection of lidocaine reduced very effectively the correlation between the CDPs for about 30 min and was practically over by 90 min.

In the experiment of Fig. 5B, the control coefficients of correlation between the CDPs were relatively high, but even so, after capsaicin there was a significant increase in the correlation, mostly between the least correlated sets of paired CDPs. This effect was transiently reverted 20 min after the administration of lidocaine. At this stage spinalization had rather mild effects on the correlation. Yet the configuration of the coefficients of correlation resembled that attained during capsaicin (RMSS=0.22).

The experiment of Fig. 5C is interesting because the control coefficients of correlation already showed a mild separation in two clusters. Capsaicin increased the correlation in the cluster comprising the weakly correlated CDPs, practically without affecting the other cluster. This effect was also temporarily reverted by lidocaine.

Changes in power spectra and coherence

Analysis of the changes in power spectra and coherence of neuronal activity during motor and cognitive processes, as well as during chronic pain, have provided relevant clues on the frequency dependence of the network activity in a variety of brain structures (see Kocsis & Vertes, 1992; Davis *et al*., 1998; Sarnthein *et al.,* 2003; Leblanc *et al*., 2014). This raised the question on the extent to which the nociceptive-induced changes in correlation between CDPs and IFPs described in the previous section were also associated with changes in power spectra and coherence of the CDPs.

Power Spectra: Fig. 6A displays the power spectra of the CDPs recorded from the caudal region in both sides of the L6 segment (L6cL, black traces and L6cR, blue traces) in the same experiment as that of Figs.1-4. It may be seen that 10-20 min after capsaicin (Fig. 6B) there was a clear increase in the power spectra of the CDPs in the low frequency range (1.5-4.5 Hz). This effect became largest by 80-90 min after the injection and was stronger on the CDPs recorded in the left (injected side) than in the right side of the spinal cord (Fig. 6C). As shown by the normalized traces in Fig. 6H, at that time capsaicin reduced the high frequency components of the power spectra.

10 to 20 minutes after the systemic administration of lidocaine, the amplitude of the power spectra was reduced and nearly recovered its pre-capsaicin values (Figs. 6D; see also normalized traces in Fig. 6I). This effect was short lasting and was over by one hour after the injection (Fig. 6E). At that time the frequency components of the power spectra were rather similar to those displayed during capsaicin (Fig. 6J). Spinalization reduced the lower frequency and increased the higher frequency components of the power spectra (Fig. 6F and 6K). A second injection of lidocaine had practically no effect on the power spectra throughout the whole frequency range (Fig. 6G and L).

The changes in power spectra produced by capsaicin and lidocaine were not restricted to one segment but comprised the whole lumbar segments in both sides of the spinal cord as illustrated in Fig. 6M-Q. Soon after the injection of capsaicin (Fig. 6N) there was a clear increase in the power spectra in the left side of the spinal cord (injection site), particularly in the rostral and caudal regions of the L6 segment. Later on, the increase in the power spectra expanded bilaterally and included the more rostral spinal segments, but even then was somewhat larger in the left than in the right side (Fig. 6O; see also Fig. 6E). The capsaicin-induced increase of the power spectra was very effectively counteracted by the systemic injection of lidocaine. This effect started around 10-20 min after the injection (Fig. 6P) and was over about one hour later (Fig. 6Q). Spinalization reduced the magnitude and segmental spread of the power spectra, particularly in the low frequency range, while at the same time increased the high frequency components (Fig. 6R). This effect was temporarily and mildly reverted by a second injection of lidocaine (Fig. 6S).

Coherence: Although the most significant effects of capsaicin and lidocaine on the power spectra of the CDPs occur in the low frequency range, they still provide limited information pertaining the frequency domains that underlie the overall changes in correlation described in the previous sections. Therefore, we examined the changes produced by capsaicin, lidocaine and spinalization on the frequency dependence of correlation. That is, on the coherence between CDPs.

Figure 6T to W discloses the effect of capsaicin and lidocaine on the coherence between the ongoing CDPs in four different frequency ranges (1.5-2.5, 3.5-4.5, 9-10 and 17.5-18.5 Hz). These frequencies correspond to the rising phase, peak and the falling phase of the power spectra (see red arrows and gray bars in Fig. 6A). Capsaicin increased the coherence, mostly in the low and intermediate frequency range (i.e., 1.5-2.5, 3.5-4.5 Hz and 9.0-10 Hz, Fig. 6T-V) and had clearly smaller effect at higher frequencies (above 17.5 Hz, Fig.6W).

As it was found for the overall correlations depicted in Fig. 1G, the systemic injection of lidocaine temporarily counteracted the effects of capsaicin on coherence in all the frequency ranges. Spinalization also reduced the coherence, particularly in the low range of frequencies (1.5-4.5 Hz). The second dose of lidocaine appeared to have a small effect, if any, on the low frequency components of the coherence, despite the clear reduction in the power spectra (see below).

In summary, analysis of effects of capsaicin on the power spectra of the CDPs recorded in each segment further indicates that the activity generated in the rostral and caudal regions of the left L6 segment is particularly affected. Coherence measurements show in addition that the stronger effects of capsaicin on correlation occur in the low frequency range, just when the power spectra attain their maximal amplitude. Similar effects were seen in the other 3 experiments included in Fig. 5 (not illustrated). The consequences of the effects of capsaicin and lidocaine on both power spectra and coherence for nociceptive responses will be further considered in the Discussion

Effects of capsaicin and lidocaine on acute spinalized preparations

Effects on correlation between paired sets of CDPs: There is a wealth of evidence pertaining the modulation of spinal neuronal activity exerted by supraspinal pathways in response to intense and prolonged nociceptive stimulation (Porreca *et al*., 2002; Vanegas & Schaible 2004; Heinricher *et al.*, 2009; Brink *et al.*, 2012).

As we have shown in the previous sections, the increased correlation between CDPs seen once the action of lidocaine was over became largely attenuated by an acute high spinal transection (see Fig. 1). This finding already indicated that the *maintenance* of the effects induced by capsaicin on the correlation between the CDPs was under supraspinal control. Yet, it raised the question on whether supraspinal influences were also required for *the establishment* of the effects of capsaicin and lidocaine, and whether this process could be prevented by previous spinalization. Such possibility might be anticipated from the findings of Urban & Gebhart (1999), who showed that spinal cord transection prevented the development of secondary, but not of primary mechanical and/or thermal hyperalgesia induced by topical mustard oil application, carrageenan inflammation or nerve section.

The raw recordings displayed in Fig. 7A and B show that spinalization reduced the slow synchronized CDPs and increased the frequency of the brief potentials recorded in the L5 and L6 segments. In contrast with what has been observed in the preparations with intact neuraxis, capsaicin applied after spinalization slightly increased the frequency of the fast components of the CDPs (Fig. 7C; see also Fig. 10A), an effect that was transiently reduced by lidocaine (Fig. 7D and E).

Fig. 7F shows that before spinalization the control coefficients of correlation of the paired sets of CDPs had a rather stable configuration that was changed after spinalization to another, also stable configuration. Following the intradermal injection of capsaicin there was a small reduction in the correlation, but later on, the distribution of the coefficients of correlation resembled that displayed before capsaicin and appeared to be slightly affected by the subsequent administration of lidocaine. Equivalent behavior was seen for the correlation between the IFPs (both superficial and deep) and the CDPs (Fig. 7G-H). In other words, *after spinalization*, neither capsaicin nor lidocaine appeared to induce major changes on the patterns of correlation between the ongoing CDPs and IFPs.

Segmental distribution of the correlation

The data depicted in Figure 8A-E show that in contrast with what has been observed in the preparation with intact neuroaxis, capsaicin and lidocaine had minor effects on the spatial (segmental) distribution of the correlation between the spontaneous CDPs when tested after spinalization. This was particularly clear for the CDPs recorded from neighboring pairs exhibiting the highest coefficients of correlation (above 0.8; Fig. 8B1-E1), but was also seen on pairs with coefficients in the 0.6-0.8 range (Fig. 8B2-E2) as well as in the lower ranges (see panels B3-E3, B4-E4 and B5-E5). It should be noted that the effects of spinalization were particularly notorious for the sets of crossed CDPs whose correlation was reduced by this procedure (compare Fig. 8A2 with Fig 8B2), a finding that suggests that crossed connectivity between dorsal horn neuronal populations is particularly affected by supraspinal influences.

Plotting the coefficients of correlation obtained during a given procedure against the control coefficients showed very clearly that spinalization led to the separation of the coefficients in two distinct clusters (Fig. 8F and G) resembling the effect of capsaicin observed in some experiments with intact neuroaxis (see Fig. 4). However in this case the effect of capsaicin and lidocaine on both clusters was rather mild (Fig. 8H-J), as it could be assessed by the relatively small changes in the slope of best linear fits of the coefficients (Ps>0.05). Yet, the RMSS values between the corresponding correlograms were of 0.4, 0.41 and 0.56, respectively, suggesting a modest resemblance between them.

Effects of capsaicin and lidocaine in other experiments

In addition to the experiment described above we examined the effects of capsaicin and lidocaine applied after acute spinalization in three additional experiments (two in Fig. 9 and one in Fig. 12). In general the results obtained agreed with those described for the experiment illustrated in Figs. 7-8. Namely, in the spinal preparation, capsaicin as well as lidocaine had rather weak effects on the intrasegmental correlation between the ongoing CDPs.

The experiment depicted in Fig. 9A is interesting because the control coefficients of correlation were rather high for all paired sets of CDPs.

Nevertheless, 30 min after spinalization there was an overall reduction in the correlation that was barely affected 20-60 min after capsaicin. The systemic injection of lidocaine (10-55 min) increased the variance of the coefficients, but even so the overall changes were not significantly different from those attained before the administration of this local anesthetic, as it could be verified by the coefficients of similarity (see Figure). As shown in the lower set of graphs, after spinalization the slopes of the best linear fits of the coefficients also remained essentially the same after capsaicin and lidocaine (Ps> 0.05).

Fig. 9B shows data from another experiment where spinalization also reduced the correlation between the CDPs and the subsequent effects of capsaicin and lidocaine were rather small. Quite interestingly, as indicated by the low coefficients of similarity, the capsaicin-induced correlograms were barely affected 20, 40 and 55 min after the systemic injection of lidocaine (RMSS= 0.24, 0.18 and 0.20, respectively). This, together with the finding that all the best linear fits had a Ps>0.05 suggests further that after spinalization the neuronal populations generating the CDPs had rather stable structured patterns of connectivity that were barely affected by capsaicin and lidocaine.

Changes in power spectra and coherence in previously spinalized preparations

Power spectra: The relatively small effects of capsaicin and lidocaine on the correlation between the CDPs observed in the spinal preparations displayed in Figs. 7 and 8 prompted us to examine the effects on their power spectra.

Spinalization reduced the power spectra in the low frequency range to about one third of control while at the same time slightly increased the high frequency components (Fig. 10A, B). In contrast with what has been observed in the preparation with intact neuraxis (Fig. 6A-C), after spinalization capsaicin produced a relatively small increase in the power spectra of the CDPs recorded in the L6rL segment, basically without affecting the power spectra of the CDPs recorded in the

637 right side (Fig. 10C), while lidocaine slightly and transiently reduced the power
638 spectra of the CDPs recorded in both sides (Fig. 10D-F).

639 Figures 10G-L illustrate the segmental distribution of the power spectra of the
640 CDPs after spinalization, capsaicin and lidocaine. They show that spinalization
641 reduced the magnitude of the power spectra in the low frequency range and at the
642 same time increased the spatial (segmental) spread of the power spectra in the
643 higher frequencies, particularly in the left side (Fig. 10H), suggesting that
644 descending influences play a relevant role in the shaping (and spatial focusing) of
645 the segmental distribution of neuronal connectivity. It should be noted that the
646 effects of capsaicin were relatively small (Fig. 10I) and included networks located
647 farther away from the primary projections of the capsaicin-activated afferents. This
648 effect was partly reversed by lidocaine, but never as it did in the preparation with
649 intact neuroaxis (Fig. 10J-L).

650 *Coherence:* The largest changes in coherence produced by spinalization were
651 observed in the low frequency range (2.5-5.0 Hz; Fig. 10M and N), but even within
652 that range the changes produced by capsaicin and lidocaine were rather small. In
653 the 9.5-10.5 Hz range capsaicin appeared to slightly reduce the correlation (Fig.
654 10O) and had almost no effects in the higher ranges (18.0-19.0 Hz; Fig. 10P).
655 Similar results were observed for the correlation and coherence of the S-IFPs and
656 D-IFPs with the CDPs recorded in this experiment (not illustrated).

657 Altogether this set of observations indicates that after acute spinalization the
658 action of capsaicin and lidocaine on the spinal networks was relatively weak in
659 comparison with that observed in preparations with intact neuroaxis. These
660 findings indicate that supraspinal influences are required not only for the
661 maintenance of the effects of capsaicin and lidocaine on the correlation between
662 the CDPs, but also for their establishment.

663 **Effects of capsaicin and lidocaine on the responses evoked by mechanical**
664 **stimulation of the skin**

Preparations with intact neuroaxis: One of the questions that emerged from the analysis of the effects of capsaicin and lidocaine on the correlation between paired sets of ongoing CDPs is the extent to which these changes had any relation with the development of secondary hyperalgesia and allodynia induced by intense and prolonged nociceptive stimulation. To this end, we examined in preparations with intact neuroaxis the effects of the intradermic injection of capsaicin and of the subsequent systemic administration of lidocaine on the spinal responses evoked by light mechanical stimulation of the skin delivered close and distant to the site of capsaicin injection (sites showing primary and secondary hyperalgesia; see Treede *et al.,*1992; Burstein *et al*., 2010; Sang *et al*., 1996) and how these changes were related to alterations in the patterns of segmental correlation between the ongoing CDPs.

In these experiments the recordings of the ongoing CDPs were briefly interrupted to stimulate the skin by means of a pair of small glass tubes connected to a device that was able to provide mechanical stimulation by delivering air puffs of controlled duration and intensity and resumed after these tests were completed (see Methods).

Figure 11A depicts the CDPs evoked in the rostral and caudal regions of the left L5 and L6 segments by mechanical stimulation of the skin with an air puff applied close to the capsaicin injection site. That is, on the region of primary hyperalgesia (Site 1). The intradermic injection of capsaicin increased both the amplitude and area of the CDPs evoked by mechanical stimulation of the skin at this site. This effect was already evident 20 min after the injection of capsaicin and became largest 75 min after the injection. At that time the amplitude of the evoked responses was increased between 128 and 148% (see 2nd column in Fig. 11A).

40 min after the injection of lidocaine the responses recorded in the L6 as well as in the rostral region of the L5 segment were further increased (144-163%), in contrast with the responses recorded in the L5cL that were slightly reduced (from 147 to 134%; 3rd column in Fig. 11A). Later on (60-85 min) the evoked responses

remained facilitated (fourth and fifth columns), suggesting a prolonged effect of capsaicin that was not reversed by lidocaine.

The effect of capsaicin and lidocaine on the segmental distribution of the CDPs produced by mechanical stimulation of the region of secondary hyperalgesia (Site 2) are illustrated in Fig. 11B. The control responses produced by the mechanical stimulus were clearly smaller than those produced by stimulation in the primary zone (see calibration bar), but even so, those recorded in the L5 segments and in the rostral region of L6 segment (L6rL) were clearly increased 75 min after the injection of capsaicin (between 109-154%; see 2nd column in Fig. 11B).

In contrast with the lack of effects of lidocaine on the capsaicin-facilitated responses produced by stimulation at site 1, 40 min after the injection of lidocaine, the amplitude of the responses recorded in the rostral and caudal region of the L5 segment and in the rostral region of the L6 segment was reduced and went below the control amplitudes (99, 78 and 82% respectively; 3rd column in Fig. 11B). By 60- 85 min the effects of lidocaine were over (4th and 5th columns in Fig. 11B).

The capsaicin-induced separation of the coefficients of correlation between the CDPs in two distinct clusters coincided in time with the increase of the CDPs evoked by mechanical stimulation of the skin, both at sites 1 and 2 (Fig. 11C, D, G and H). An unexpected and quite interesting finding was that the lidocaine-induced merging of the coefficients in one cluster (Fig. 11E, I) occurred during the reversion of the capsaicin-induced facilitation of the CDPs evoked by mechanical stimulation at site 2. Furthermore, the subsequent increase in the mechanically evoked responses observed after the lidocaine effects were over, again coincided with the separation of the coefficients in two clusters (Fig. 11F, J) suggesting a persistent action of capsaicin.

Effects in previously spinalized preparations: The observations described in Figs. 7-10 already indicated that in previously spinalized preparations capsaicin and lidocaine had rather small effects on the correlation between the ongoing CDPs. It thus seemed important to examine the effects of these procedures on the responses evoked after spinalization by mechanical stimulation of the skin.

724 The first column in Fig. 12A shows the responses recorded in several spinal
725 segments following a mechanical stimulus applied rather close to the site of the
726 injection of capsaicin in the footpad (Site 1). The largest responses were generated
727 in the caudal region of the left L6 segment (L6cL) and in the rostral part of the L7
728 segment (not illustrated). After spinalization the responses recorded in L6cL
729 following tactile stimulation were facilitated to 116% relative to control and
730 remained about the same in the other segments (2nd column in Fig. 12A). 65 min
731 after the intradermic injection of capsaicin in the already spinalized preparation, the
732 amplitude of the evoked responses recorded in all segments was clearly smaller
733 (from 58 to 77% relative to the amplitude of the responses recorded after
734 spinalization; see 3rd column Fig. 12A) and increased again after lidocaine (4th and
735 5th columns in Fig. 12A).

736 After spinalization, the responses produced in segments L5 and L6 by
737 mechanical stimulation applied to the region of secondary hyperalgesia (Site 2)
738 showed relatively small changes when tested 65 min after capsaicin except in
739 segment L5cL that were reduced to 83% (compare 2nd and 3rd columns in Fig.
740 12B). The subsequent injection of lidocaine slightly reduced the responses evoked
741 in the L5 segment and had a rather small effect on the responses evoked in the L6
742 segment (4th and 5th columns in Fig. 12B).

743 As in Fig. 8G, spinalization separated the coefficients of correlation in two
744 clusters (Fig. 12C, D, H and I). 70-75 min after capsaicin there was a clear
745 reduction in the correlation of the paired set of CDPs included in cluster C2,
746 practically without affecting the correlation between the CDPs included in cluster
747 C1 (Fig. 12 E and J). The slopes of the best fits of the C1 and C2 clusters obtained
748 after capsaicin remained basically the same 15-20 min and 40-45 min after
749 lidocaine (Ps>0.05; Fig. 12F,G,K,L), even though the correlograms obtained after
750 capsaicin (Fig. 12E) and Lidocaine 15-20min (Fig. 12F) were somewhat different
751 (RMSS=0.74).

752 In summary, these observations indicate that the effects of capsaicin and
753 lidocaine on the segmental correlation between paired sets of ongoing CDPs as

well as on the CDPs evoked by mechanical stimulation of the skin in the region of secondary hyperalgesia are relatively small when these tests are performed in preparations previously devoid of supraspinal influences.

Discussion

The present observations have shown a) that the intradermic injection of capsaicin in the left hind paw increases the coefficients of correlation between the ongoing cord dorsum potentials simultaneously recorded from different lumbar spinal segments as well as their correlation with the superficial and deep intraspinal field potentials, b) the effects of capsaicin on these correlations are transiently counteracted by the systemic administration of a small dose of lidocaine, c) the effects of capsaicin and lidocaine on the correlation between CDPs as well as on the cord dorsum responses evoked by mechanical stimulation of the skin in the region of secondary hyperalgesia are greatly attenuated when tested in previously spinalized preparations.

Altogether the present findings are taken as an indication that capsaicin induces a structured, non-random (see Methods) supraspinally mediated reorganization of the functional connectivity between the spinal neuronal networks involved in the generation of the ongoing CDPs that is transiently reversed by lidocaine. Similar increases in correlation between CDPs as those exerted by capsaicin and lidocaine have been observed with skin lesions produced by localized burning (unpublished observations).

The action of Capsaicin and lidocaine on neuronal correlation

The intradermic injection of capsaicin induces inflammatory nociception through the activation of the VR1 receptors in the A∂ and C fibres innervating the affected skin areas and increases their synaptic effectiveness (Hui *et al*., 2003) as well as mechanical hyperalgesia in humans (Wallace *et al*., 1997; Holthusen *et al*., 2000). The timing of the long lasting increase in correlation and coherence between cord dorsum potentials induced by intradermal capsaicin suggests that this effect is not related to the initial short lasting activation of C-fiber nociceptors that follows the

783 intradermic injection (Wall & Woolf, 1984; Cook *et al*., 1987), but to enduring
784 central influences, since the maximum effects of capsaicin are seen about 90
785 minutes after the intradermic injection, while the capsaicin-induced increase in the
786 C fiber activity lasts less than 60 minutes and is followed by inhibition (Galhardo *et*
787 *al*., 2002). Moreover, after the central effect of capsaicin has been established,
788 local anesthesia of the inflamed paw produced no substantial changes on the
789 capsaicin-induced changes in correlation between CDPs (unpublished
790 observations).

791 The slight reduction in correlation observed during the first 10 minutes after the
792 injection of capsaicin shown in Fig. 1G could be due to a short-lasting capsaicin
793 induced inhibition of the synaptic actions of the nociceptive afferents in the dorsal
794 horn (Yanga *et al*., 1999). It is also possible that the desynchronized barrage of
795 sensory input produced by this nociceptive stimulus temporarily counteracts the
796 correlation between CDPs (see Inbar *et al*., 1979).

797 Pertaining the effect of lidocaine, Puig & Sorkin (1996) showed that the effects
798 of systemic injection of lidocaine were not related to blockade of impulse
799 conduction in low threshold tactile afferents, although they could silence the A∂ and
800 C fibres already activated by the nociceptive stimulus. These findings agree with
801 our observation that the systemic administration of a low dose of lidocaine had no
802 anesthetic effect on the peripheral and intraspinal terminals of low threshold
803 afferents since it did not depress the cord dorsum responses produced by
804 mechanical stimulation of the skin at the site of the primary hyperalgesia produced
805 by the injection of capsaicin (Fig. 11A).

806 Alternatively, lidocaine could have a direct effect on the capsaicin-activated
807 nociceptive afferents as well as on the spinal neurones affected by capsaicin. It
808 could also act as an anesthetic onto the supraspinal networks and reduce their
809 influence on the spinal neuronal activity in response to the nociceptive stimuli.
810 Although these possibilities are not mutually exclusive, a relevant supraspinal
811 action is supported by the finding that the capsaicin-induced increase in the
812 correlation between the spinal networks and its temporal reversal by lidocaine are

minimal when capsaicin and lidocaine are administered in previously spinalized preparations (Figs.7-10 and Fig. 12; for review see Urban & Gebhart 1999).

We suggest that the intradermic injection of capsaicin activates ascending nociceptive pathways (most likely via the lateral spinothalamic pathway) that trigger supraspinally mediated changes. The state of central sensitization induced by the nociceptive stimulus would be transiently curtailed by lidocaine acting most likely on supraspinal neurones in the periaqueductal gray (PAG) which is a relay of ascending and descending nociceptive pathways, as well as in the ventromedial medulla (RVM) and raphe nuclei, among others (see Willis, 1985; Jones & Gebhart, 1987; Zhuo & Gebhart, 1997; Urban & Gebhart, 1999; Fields 2000; Millan, 2002; Suzuki and Dickenson, 2005).

Nociceptive-induced coupling between supraspinal and spinal activity?

There is a wealth of information showing that many central structures display delta and theta waves during nociception both in animal models (Miletic & Coffield, 1989; Kocsis & Vertes, 1992; Leblanc *et al*., 2014) and in humans under different neurological conditions as well as during neuropathic pain (Sarnthein & Jeanmonod, 2008). Our data indicate that in the preparations with intact neuroaxis the capsaicin-induced increase in coherence between spinal neuronal activity also occurs within this range, that is also the range of activity observed in spinalized preparations, even before the injection of capsaicin.

It is tempting to suggest that spinal and supraspinal oscillations at similar frequency rates provide the temporal structure that allows them to enter in resonance (Fries, 2005), a feature of relevance for the shaping of the nociceptive message (Katz *et al*., 1999; Averbeck & Lee., 2004; Shyu & Vogt, 2009) and for pain perception (Burstein *et al*., 2010).

Supraspinal control of allodynia and secondary hyperalgesia

Our observations indicate that during the state of central sensitization induced by capsaicin there is a significant increase in the correlated activity of superficial and deep IFPs with the CDPs (Fig. 3). This effect occurs on both sides of the

842 spinal cord, is larger between the deep IFPs (laminae III-V) and CDPs than
843 between the superficial IFPs (laminae I and II) and CDPs at the segmental level of
844 entrance of nociceptive information in the ipsilateral (left) side, and gradually
845 expands in a rostral and caudal direction on both sides of the cord.

846 This fits very well with the observations of Schoffnegger *et al*., (2008) who
847 showed that allodynia (pain elicited by innocuous stimuli), is associated with a
848 synaptically mediated spread of excitation from deep intraspinal areas of
849 termination of Aβ fibers (laminae III-V) to the superficial dorsal horn (laminae I and
850 II; see also Willis & Coggeshall, 2004), and partly explains the finding of Levine *et*
851 *al*., (1985) who showed in rats that capsaicin injected in one hindlimb induced
852 hyperalgesia and edema on both ipsi and contrateral hindlimbs, possibly through a
853 supraspinal neural action.

854 These findings, together with the observation that the capsaicin-induced
855 increase in the amplitude of the CDPs produced by mechanical stimulation of the
856 skin in the region of secondary hyperalgesia occurred in association with a state of
857 increased correlation between CDPs, while the reduction of the capsaicin-induced
858 facilitation of the evoked potentials that followed the administration of lidocaine
859 happened during the state of decreased correlation between CDPs (Fig. 11), are
860 compatible with a causal relation between the changes in correlation of the CDP-
861 generating neuronal ensembles and the changes in the responses produced by
862 mechanical stimulation of the skin. An additional argument supporting this proposal
863 is that both require the connection of the spinal neuronal networks with supraspinal
864 structures (Fig. 12).

865 **Some functional implications**

866 The present set of observations suggests that the changes in functional
867 connectivity between spinal neurones produced by acute nociceptive stimulation
868 are the expression of the dynamic response of a system in conditions of criticality
869 in which descending control is able to shift the neuronal networks to a different
870 functional state. That is, of a self-organized system in a critical state where minor

disturbances in neuronal synchronization may lead to events way out of balance (Bak, 1997; Parker & Srivastava, 2013; Haimovici *et al*., 2013, Hesse & Gross, 2014; Massobrio *et al*., 2015).

The tempering of this state by systemic lidocaine correlates well with clinical observations in humans and provides further evidence that descending supraspinal influences operating on the spinal cord are part of the process of central sensitization which persists once it has been established (pain memory?; see Vera-Portocarrero *et al*., 2006; Smith *et al*., 2002; Bee & Dickenson 2007, 2008).

One important question that remains to be addressed is how the observed effects of capsaicin and lidocaine are brought about. Are the capsaicin induced changes product of the activation of a limited repertoire of structured configurations of tightly coupled sets of neurones (modules?) (see Song *et al*., 2005; d'Avella & Bizzi, 2005) or else, are these configurations produced by graded changes in neuronal connectivity within the same distributed ensemble, as suggested by the observations of Contreras-Hernández *et al*., (2015).

Structured changes in synchronization between dorsal horn neurones appear to be an effective way to address information flow to specific neuronal networks (see also Abarbanel *et al*., 1996; Jiao, 2006; Womelsdorf *et al*., 2007). In fact, the recruitment of presynaptic inhibitory pathways during high levels of spontaneous dorsal horn neuronal synchronization described by Contreras-Hernández *et al.*, (2015), could play a relevant role in the addressing of sensory information during secondary hyperalgesia and allodynia induced by nociceptive stimulation (see Cervero *et al*., 2003).

The present study provides important evidence regarding the overall changes in neuronal correlation during nociceptive stimulation but rather limited information on the concurrent changes in the connectivity of specific, functionally identified neuronal populations. Based on the assumption that the spontaneous CDPs are produced by the synchronous activation of specific populations of dorsal horn neurones (Manjarrez *et al*., 2000, 2003; Chávez *et al*., 2012), one possible approach to this problem would be to examine the changes induced by nociceptive

stimulation on the different types of spontaneous CDPs and relate them to a specific function as it was recently done by Contreras-Hernández *et al*. (2015).

To this end, we developed a machine learning procedure for the automatic selection of the ongoing CDPs according to their shape and amplitude (Martín *et al*., 2015). With this method the CDPs recorded in a particular experiment during different procedures could be reliably separated in different classes. We found that the classes comprising the smallest CDPs had higher probabilities of occurrence than those including the largest CDPs. We also found that capsaicin had a dual action on the CDPs. Namely, it reduced the probabilities of occurrence of some of the small CDP classes while at the same time increased the probabilities of occurrence of most of the largest CDP classes. These changes led to a different non-random configuration of the whole set of CDPs that was fully and temporarily reversed by lidocaine (Rudomin *et al*., 2012). These differential effects of capsaicin on the CDPs could also contribute to the assemblage of the coefficients of correlation in two distinct clusters (Figs. 3 and 4). The finding that spinalization also separates the coefficients in two classes (Fig. 8G) further suggests that the single cluster arrangement depends, to a great extent, on supraspinal influences that are disrupted by capsaicin.

To fully appreciate the functional implications of the supraspinal modulation of the effects of capsaicin on the different classes of CDPs it is necessary to examine the association of each class with a specific function (e.g. with the generation of DRPs and presynaptic inhibition), as well as their correlation with the activity of individual, functionally identified neurones (see Contreras-Hernández *et al.,* 2015). A detailed characterization of the genetic identity of the neurones contributing to the different classes of CDPs could also contribute to this endeavor (see Zagoraiou *et al*., 2009; Goulding 2009; Fink *et al*., 2014).

A final point: Changes in the ongoing cord dorsum activity have been occasionally used to evaluate disorders in patients with peripheral nerve, root and spinal cord damage (Ertekin *et al*., 1983), to monitor changes in spinal cord activity during microsurgical sectioning of dorsal roots for pain, spasticity and hyperactive bladder (Sindou *et al*., 1994) and also to predict harmful spinal cord ischemia

during repair of thoracic or thoraco-abdominal aortic aneurysms (Stuhmeier *et al*., 1993). We believe that information obtained from the changes in correlation between ongoing CDPs may provide useful indicators of the functional states of the spinal cord in humans under diverse normal and pathological situations.

Additional information

Competing interests

None declared

Author contributions

Conception and design of experiments: RP, GS, ChD, CHE
Conduction of the experiments ChD, CHE, GS, CHE, PR
Collection and interpretation of data: RP, GS, CHE, ChD.
Programming and data analysis CHE, VE, ReP, BJ, MM & CU
Drafting of the article and reviewing it critically for important intellectual content: RP, GS, CHE, ChD, CU**.**
Experiments were performed at the Department of Physiology, Biophysics and Neurosciences, Center of Research and Advanced Studies of the Instituto Politécnico Nacional, México.
All authors approved the final version of the manuscript for publication.

Funding

This work was partly supported CONACyT grants 50900 and 255548 and Fondo Jaime Torres Bodet SEP, México (ECN-JTB2017). CHE was holder of a CONACyT fellowship for doctoral studies.

Acknowledgements

We would like to thank Dr. H Vanegas for his comments to an earlier version of this paper, to A Ramírez for his participation in some experiments, to L Moreno for his help with statistical analysis of the data, to C León for technical assistance and to E Rosales for her excellent secretarial support.

960 REFERENCES

961 Abaei M, Sagar DR, Stockley EG, Spicer CH, Prior M, Chapman V & Auer DP
962 (2016). Neural correlates of hyperalgesia in the monosodium iodoacetate model of
963 osteo-arthritis pain. *Mol Pain* **12**, 1744806916642445.

964 Abarbanel HDI, Rabinovich MI, Selverston A, Bazhenov MV, Huerta R, Sushchik
965 MM & Rubchinskii LL (1996). Synchronization in neural networks. *Physics-Uspekhi*
966 **39**, 337–362.

967 Averbeck BB & Lee D (2004). Coding and transmission of information by neural
968 ensembles. *Trends Neurosci* **27**, 225–230.

969 Bak P (1997). How Nature Works: The Science of Self-organized Criticality. Oxford
970 University Press, Oxford, UK.

971 Basbaum A, Bautista DM, Scherrer G & Julius D (2009). Cellular and Molecular
972 Mechanisms of Pain. *Cell* **139**, 267-284.

973 Bee LA & Dickenson AH (2007). Rostral ventromedial medulla control of spinal
974 sensory processing in normal and pathophysiological states. *Pain* **147**, 786-793.

975 Bee LA & Dickenson AH (2008). Descending facilitation from the brainstem
976 determines behavioural and neuronal hypersensitivity following nerve injury and
977 efficacy of pregabalin. *Pain* **140**, 209-223.

978 Biella G, Riva L & Sotgiu ML (1997). Interaction between neurons in different
979 laminae of the dorsal horn of the spinal cord. A correlation study in normal and
980 neuropathic rats. *Eur J Neurosci* **9**, 1017-1025.

981 Bityukov S, Krasnikov N, Nikitenko A &, Smirnova V (2013). A method for statistical
982 comparison of histograms. arXiv: 1302.2651

983 Bonin RP & De Koninck Y (2014). A spinal analog of memory reconsolidation
984 enables reversal of hyperalgesia. *Nat Neurosci* **17**, 1043–1045.

985 Brink TS, Pacharinsak C, Khasabov SG, Beitz AJ & Simone DA (2012). Differential
986 modulation of neurons in the rostral ventromedial medulla by neurokinin-1
987 receptors. *J Neurophysiol* **107**, 1210–1221.

988 Burstein R, Jakubowski M, Garcia-Nicas E, Kainz V, Bajwa Z, Hargreaves R &
989 Becerra L (2010). Thalamic sensitization transforms localized pain into widespread
990 allodynia. *Ann Neurol* **68**, 81–91.

991 Cervero F, Laird JMA & García-Nicas E (2003). Secondary hyperalgesia and
992 presynaptic inhibition: an update. *Eur J Pain* **7**, 345–351.
993 Challapalli V, Tremont-Lukats IW, McNicol ED, Lau J & Carr DB (2005). Systemic
994 administration of local anesthetics agents to relieve neuropathic pain. Cochrane
995 Pain, Palliative and Supportive Care Group, John Wiley & Sons, Lt.
996 Chávez D, Rodríguez E, Jiménez I & Rudomin P (2012). Changes in correlation
997 between ongoing activity of dorsal horn neurones lead to differential recruitment of
998 inhibitory pathways in the cat spinal cord. *J Physiol* **590**, 1563-1584.
999 Chen LM, Mishra A, Yang PF, Wang F & Gore JC (2015). Injury alters intrinsic
1000 functional connectivity within the primate spinal cord. *Proc Natl Acad Sci USA* **112**,
1001 5991-5996.
1002 Contreras-Hernández E, Chávez D & Rudomin P (2015). Dynamic synchronization
1003 of ongoing neuronal activity accross spinal segments regulates sensory information
1004 flow. *J Physiol* **593**, 2343-2363.
1005 Contreras-Hernández E, Chávez D, Hernández E, Glusman S & Rudomin P
1006 (2013). Reorganization of functional connectivity between dorsal horn neuronal
1007 networks produced by intradermic capsaicin and heat-induced skin damage and its
1008 transient restoration by systemic lidocaine. *Abs Soc Neurosci* **645.03**.
1009 Cook AJ, Woolf CJ, Wall PD & McMahon SB (1987). Dynamic receptive field
1010 plasticity in rat spinal cord dorsal horn following C primary afferent input. *Nature*
1011 **325**, 151-153.
1012 d'Avella A & Bizzi E (2005). Shared and specific muscle synergies in natural motor
1013 behaviors. *Proc Natl Acad Sci USA* **102**, 3079-3081.
1014 Davis K D, Kwan CL, Crawley AP & Mikulis DJ (1998). Functional MRI study of
1015 thalamic and cortical activations evoked by cutaneous heat, cold, and tactile
1016 stimuli. *J Neurophysiol* **80**, 1533-1546.
1017 Dirks J, Peder F, Fabricius P, Petersen KL, Rowbotham MC & Dahl JB (2000). The
1018 effect of systemic lidocaine on pain and secondary hyperalgesia associated with
1019 the heat/capsaicin sensitization Model in healthy volunteers. *Anesth Analg*, **91**,
1020 967–972.

1021 Drdla-Schutting R, Benrath J, Wunderbaldinger G & Sandkuhler J (2012). Erasure
1022 of a spinal memory trace of pain by a brief high-dose opioid administration.
1023 *Science* **335**, 235-238.
1024 Eblen-Zajjur A A & Sandkühler J (1996). Synchronicity of nociceptive and non-
1025 nociceptive adjacent neurons in the spinal dorsal horn of the rat: stimulus-induced
1026 plasticity. *Neuroscience* ***76***, 39-54.
1027 Endo T, Spenger Ch, Westman E, Tominaga T & Olson L (2008). Reorganization
1028 of sensory processing below the level of spinal cord injury as revealed by fMRI.
1029 *Exp Neurol* **209**, 155–160.
1030 Ertekin C, Sarica Y & Ückardesler L (1983). Studies on the human ongoing
1031 electromyelogram (EMyeloG). II. Patients with peripheral nerve, root and spinal
1032 cord disorders. *EEG Clin Neurophysiol* **55**, 24-33.
1033 Fields HL (2000) Pain modulation: expectations, opioid analgesia and virtual pain.
1034 *Prog Brain Res* 122, 245-253.
1035 Fields HL (2004). State-Dependent opiod control of pain. *Nat Rev Neurosci* **5**, 565-
1036 575.
1037 Fink AJP, Croce KR, Huang ZJ, Abbott LF, Jessell TM & Azim E (2014).
1038 Presynaptic inhibition of spinal sensory feedback ensures smooth movement.
1039 *Nature* **509**, 43–48.
1040 Fries P (2005). A mechanism for cognitive dynamics: neuronal communication
1041 through neuronal coherence. *Trends Cog Sci* **9**, 474–480.
1042 Galhardo V, Apkarian AV & Lima D (2002). Peripheral Inflammation Increases the
1043 Functional Coherency of Spinal Responses to Tactile but not Nociceptive
1044 Stimulation. *J Neurophysiol* 88, 2096-2103.
1045 Gibbons JD (1996). Non-parametric Methods for Quantitative Analysis, 3rd edition.
1046 American Science Press, Inc.
1047 Gordon D & Schroeder M (2008). Intravenous lidocaine for postoperative
1048 analgesia: renewed Interest in an old strategy. *Am Pain Soc Bull* **18**, 3-5.
1049 Goulding M (2009). Circuits controlling vertebrate locomotion: moving in a new
1050 direction. *Nat Rev Neurosci* **10**, 507-518.

1051 Grundy D (2015) Principles and standards for reporting animal experiments in The
1052 Journal of Physiology and Experimental Physiology *J Physiol*, **593:** 2547-2549.
1053 doi:10.1113/JP270818.
1054 Haimovici A, Tagliazucchi E, Balenzuela P & Chialvo DR (2013). Brain
1055 organization into resting state networks emerges at criticality on a model of the
1056 human connectome. *Phys Rev Lett* **110**, 178101.
1057 Heinricher MM, Tavares I, Leith JL & Lumb BM (2009). Descending control of
1058 nociception: specificity, recruitment and plasticity. *Brain Res Rev* **60**, 214-225.
1059 Hesse J & Gross T (2014). Self-organized criticality as a fundamental property of
1060 neural systems. *Front Syst Neurosci* **8**, 166.
1061 Holthusen H, Irsfeld S & Lipfert P (2000) The effect of pre- and post-traumatically
1062 applied i.v. lidocaine on primary and secondary hyperalgesia after experimental
1063 heat trauma in humans. *Pain* 88, 295-302).
1064 Hui K, Liu B, & Qin F (2003). Capsaicin activation of the pain receptor, VR1:
1065 multiple open states from both partial and full binding. *Biophys J* **84**, 2957-2968.
1066 Inbar G, Madrid J and Rudomin P (1979). The influence of the gamma system on
1067 cross-correlated activity of Ia muscle spindles and its relation to information
1068 transmission. *Neuroscience Letters* 13, 73-78.
1069 Jiao X & Wang R (2006). Synchronization in neuronal population with the variable
1070 coupling strength in the presence of external stimulus. *App Phys Lett* **88**, 203901.
1071 Jones SL & Gebhart GF (1987). Spinal pathways mediating tonic, coeruleospinal,
1072 and raphe-spinal descending inhibition in the rat. *J Neurophysiol* **58**, 138-159.
1073 Kaas JH (1991). Plasticity of sensory and motor maps in adult mammals. *Annu*
1074 *Rev Neurosci* **14**, 137-167.
1075 Katz DB, Simon SA, Moody A & Nicolelis MA (1999). Simultaneous reorganization
1076 in thalamocortical ensembles evolves over several hours after perioral capsaicin
1077 Injections. *J Neurophysiol* **82**, 963-977.
1078 Kocsis B & Vertes RP (1992). Dorsal raphe neurons: synchronous discharge with
1079 the theta rhythm of the hippocampus in the freely behaving rat. *J Neurophysiol* **68**,
1080 1463-1467.

1081 Latremoliere A & Woolf CJ (2009). Central sensitization: a generator of pain
1082 hypersensitivity by central neural plasticity. *J Pain* **10**, 895-926.
1083 LeBlanc BW, Lii TR, Silverman AE, Alleyne RT & Saab CY (2014). Cortical theta is
1084 increased while thalamocortical coherence is decreased in rat models of acute and
1085 chronic pain. *Pain* **155**, 773–782.
1086 Levine JD, Dardick SJ, Basbaum AI & Scipio E (1985) Reflex Neurogenic
1087 inflammation I. Contribution of the peripheral nervous system to spatially remote
1088 inflammatory responses that follow injury. *J Neurosci* **5**,1380-1386.
1089 Malliani A, Rudomin P & Zanchetti A (1965) Contribution of local activity and
1090 electrical spread to somatically evoked potentials in different areas of the
1091 hypothalamus. *Arch Ital Biol* ***103***, 119-135.
1092 Manjarrez E, Jiménez I & Rudomin P (2003). Intersegmental synchronization of
1093 ongoing activity of dorsal horn neurons in the cat spinal cord. *Exp Brain Res* **148**,
1094 401- 413.
1095 Manjarrez E, Rojas-Piloni JG, Jiménez I & Rudomin P (2000). Modulation of
1096 synaptic transmission from segmental afferents by ongoing activity of dorsal horn
1097 spinal neurons in the cat. *J Physiol* **529**, 445-460.
1098 Mao J & Chen LL (2000). Systemic lidocaine for neuropathic pain relief. *Pain* **87**, 7-
1099 17.
1100 Martín M, Contreras-Hernández E, Béjar J, Esposito G, Chávez D, Glusman S,
1101 Cortés U & Rudomin P (2015). A machine learning methodology for the selection
1102 and classification of ongoing cord dorsum potentials allows disclosure of structured
1103 (non-random) changes in neuronal connectivity induced by nociceptive stimulation.
1104 *Front Neuroinform* **9**, 21.
1105 Massobrio P, de Arcangelis L, Pasquale V, Jensen HJ & Plenz D (2015). Criticality
1106 as a signature of healthy neural systems. *Front Syst Neurosci* **9**, 22.
1107 McDonald JH (2014). Handbook of Biological Statistics (3rd ed.). Sparky House
1108 Publishing, Baltimore, Maryland.
1109 Miletic V & Coffield JA (1989). Responses of neurons in the rat nucleus submedius
1110 to noxious and innocuous mechanical cutaneous stimulation. *Somatosens Mot Res*
1111 **6**, 567-587.

1112 Millan MJ (2002) Descending control of pain*. Prog Neurobiol* 66, 355-474.
1113 Obien MEJ, Deligkaris K, Bullmann T, Bakkum DJ & Frey U (2015). Revealing
1114 neuronal function through microelectrode array recordings. *Front Neurosci* **8**, 423.
1115 Parker D & Srivastava V (2013). Dynamic systems approaches and levels of
1116 analysis in the nervous system. *Front Physiol* **4**, 15.
1117 Pettit MJ & Schwark HD (1996). Capsaicin-induced rapid receptive field
1118 reorganization in cuneate neurons. *J Neurophysiol* **75**, 1117-1125.
1119 Porreca F, Ossipov MH & Gebhart GF (2002). Chronic pain and medullary
1120 descending facilitation. *Trends Neurosci* **25**, 319-325.
1121 Puig S & Sorkin LS (1996). Formalin-evoked activity in identified primary afferent
1122 fibers: systemic lidocaine suppresses phase-2 activity. *Pain* **64**, 345–355.
1123 Roza C, Mazo I, Rivera-Arconada I, Cisneros E, Alayón I & López-García JA
1124 (2016). Analysis of ongoing activity of superficial dorsal horn neurons in vitro:
1125 neuropathy- induced changes. *Pflugers Arch-Eur J Physiol* **468**, 2017-2030.
1126 Rudomin P & Hernández E (2008). Changes in synaptic effectiveness of
1127 myelinated joint afferents during capsaicin-*induced inflammation of the footpad in*
1128 *the anesthetized cat. Exp Brain Res* **187**, 71-84.
1129 Rudomin P, Chávez D, Contreras-Hernández E, Rodríguez E, Hernández E &
1130 Glusman S (2012). Systemic lidocaine transiently restores disruption of functional
1131 connectivity between dorsal horn neuronal ensembles produced by capsaicin-
1132 induced skin inflammation. *Abs Soc Neurosci* **179.20**.
1133 Sakurada T, Katsumata K, Tan-No K, Sakurada S & Kisara K (1992). The
1134 capsaicin test in mice for evaluating tachykinin antagonists in the spinal cord.
1135 *Neuropharmacol* **31**, 1279-1285.
1136 Sandkuler J (2007). Understanding LTP in pain pathways. *Mol Pain* **3**, 9.
1137 Sandkuhler J (2009). Models and mechanisms of hyperalgesia and allodynia.
1138 *Physiol Rev* **89**, 707-758.
1139 Sang CN, Gracely RH, Max MB & Bennett GJ (1996). Capsaicin-evoked
1140 mechanical allodynia and hyperalgesia cross nerve territories. Evidence for a
1141 central mechanism. *Anesthesiol* **85**, 491-496.

Sarnthein J and Jeanmonod D (2008). High thalamocortical theta coherence in patients with neurogenic pain. *Neuroimage* **39**, 1910–1917.

Sarnthein J, Morel A, von Stein A and Jeanmonod D (2003). Thalamic theta field potentials and EEG: high thalamocortical coherence in patients with neurogenic pain, epilepsy and movement disorders. *Thalamus Relat Sys* **2**, 231-238.

Schaible HG, Schmidt RF & Willis WD (1987). Enhancement of the responses of ascending tract cells in the cat spinal cord by acute inflammation of the knee joint. *Exp Brain Res* **66**, 489-499.

Schoffnegger, D, Ruscheweyh R & Sandkuhler J (2008) Spread of excitation across modality borders in spinal dorsal horn of neuropathic rats. *Pain* **135**, 300-310.

Shyu BC & Vogt BA (2009). Short-term synaptic plasticity in the nociceptive thalamic-anterior cingulate pathway. *Mol Pain* **5**, 51.

Sindou M, Turano G, Pantieri R, Mertens P & Mauguiere F (1994). Intraoperative monitoring of spinal cord SEPs during microsurgical. *Stereotac Funct Neurosurg* **62**, 164-170.

Smith LJ, Shih A,. Miletic G, Miletic V (2002). Continual systemic infusion of lidocaine provides analgesia in an animal model of neuropathic pain. *Pain* **97**, 267-273.

Song S, Sjostrom PJ, Reigl M, Nelson S & Chklovskii DB (2005). Highly nonrandom features of synaptic connectivity in local cortical circuits. *PLoS Biol* **3**, e68.

Sotgiu ML, Valente M, Storchi R, Caramenti G & Biella GE (2009). Cooperative N-methyl-D-aspartate (NMDA) receptor antagonism and mu-opioid receptor agonism mediate the methadone inhibition of the spinal neuron pain-related hyperactivity in a rat model of neuropathic pain. *Pharmacol Res* **60**, 284-290.

Stuhmeier KD, Grabitz K, Mainzer B, Sandmann W & Tarnow J (1993). Use of the electrospinogram for predicting harmful spinal cord ischemia during repair of thoracic or thoracoabdominal aortic aneurysms. *Anesthesiol* **79**, 1170-1176.

Suzuki R & Dickenson A (2005) Spinal and supraspinal contributions to central sensitization in peripheral neuropathy. *Neurosignals* 14: 175-181.

Treede RD, Meyer RA, Raja SN & Campbell JN (1992). Peripheral and central mechanisms of cutaneous hyperalgesia. *Prog Neurobiol* **38**, 397– 421.

Tremont-Lukats IW, Hutson PR & Backonja MM (2006). A randomized, double-masked, placebo-controlled pilot trial of extended IV lidocaine infusion for relief of ongoing neuropathic pain. *Clin J Pain* **22**, 266-271.

Urban MO & Gebhart GF (1999). Supraspinal contributions to hyperalgesia. *Proc Natl Acad Sci USA* **96**, 7687-7692.

Vanegas H & Schaible HG (2004). Descending control of persistent pain: inhibitory or facilitatory? *Brain Res Rev* **46**, 295-309.

Vera-Portocarrero LP, Zhang ET, Ossipov MH, Xie JY, King T, Lai J & Porreca F (2006). Descending facilitation from the rostral ventromedial medulla maintains nerve injury-induced central sensitization. *Neurosci* **140**, 1311-1320.

Yanga K, Kumamotoa E. Furuea H, Lib YQ & Yoshimuraa M (1999) Action of capsaicin on dorsal root-evoked synaptic transmission to substantia gelatinosa neurons in adult rat spinal cord slices. *Brain Res* **830**, 268-273.

Wall PD & Werman R (1976). The physiology and anatomy of long ranging afferent fibres within the spinal cord. *J Physiol* **255**, 321-334.

Wall PD & Woolf C J (1984). Muscle but not cutaneous C-afferent input produces prolonged increases in the excitability of the flexion reflex in the rat. *J Physiol* **356**, 443-458.

Wall PD, Kerr BJ & Ramer MS (2002). Primary afferent input to and receptive field properties of cells in rat lumbar area X. *J Com Neurol* **449**, 298-306.

Wallace MS, Laitin S, Licht D & Yaksh TL (1997). Concentration-effect relations for intravenous lidocaine infusions in human volunteers: Effects on acute sensory thresholds and capsaicin-evoked hyperpathia. *Anesthesiol **86***, 1262-1272.

Willis WD (1985). Nociceptive pathways: min

Woolf CJ (2007). Central sensitization: uncovering the relation between pain and plasticity. *Anesthesiol* **106**, 864–867.

Womelsdorf T, Schoffelen JM, Oostenveld R, Singer W, Desimone R, Engel AK & Fries P (2007). Modulation of neuronal interactions through neuronal synchronization. *Science* **316**, 1609-1612.

Zagoraiou L, Akay T, Martin JF, Brownstone RM, Jessell TM & Miles GB (2009). A Cluster of cholinergic premotor interneurons modulates mouse locomotor activity. *Neuron* **64**, 645–662.

Zhuo M, Gebhart G (1997) Biphasic modulation of spinal nociceptive transmission from the medullary raphe nuclei in the rat. *J. Neurophysiol* **78**,746-758.

Figure Legends

Figure 1.- Systemic lidocaine reverses the capsaicin-induced increase in correlation between ongoing spinal cord activity. A-F, CDPs recorded from the L5 caudal and the L6 rostral segments in both sides and IFPs recorded at two different depths in the L6cL segment before and after capsaicin, lidocaine and spinalization, as indicated. Negativity is upward for CDPs and downward for the IFPs. The histological section on the left shows the intraspinal location of the IFP recording sites. **G**, changes produced by capsaicin, lidocaine and spinalization on the correlation between the paired sets of CDPs recorded with the ensemble of 12 electrodes placed along the L4-L7 segments on both sides of the spinal cord. The whole set of coefficients of correlation obtained during the 10 min Control 0 recording period is displayed in descending order as a vertical column. The coefficients of correlation obtained from 10 min non-overlapping recordings made at subsequent times are displayed keeping the same order as the Control 0 coefficients. Colors show magnitude of correlation (see scale). Arrows show time of capsaicin and lidocaine injections and of spinalization. **H-I,** equivalent displays of the coefficients of correlation of the S-IFPs and D-IFPs with the CDPs recorded from different segments, as indicated. See text for further explanations.

Figure 2.- The patterns of segmental correlation between CDPs are disrupted after the intradermic injection of capsaicin and temporarily restored by systemic lidocaine. A, horizontal display of the coefficients of correlation obtained from all the combinations between paired sets of the CDPs recorded during the control period ordered according to their magnitude and separated in 4 different ranges as shown by colors. **A1-A4**, spinal cord diagrams showing the segmental location of the paired sets of CDPs used to calculate the coefficients of correlation in each range. Lines indicate segmental location of CDP recording sites. **B-B4**, correlograms and segmental distribution of coefficients obtained from recordings made 70-80 min after the injection of capsaicin. Note in panel B1 increased correlation between CDPs recorded from neighboring segments. **C-C4**, the effects

of capsaicin are reversed 10-20 min after the systemic injection of lidocaine. **D-D4**, restoration of the effects of capsaicin 80-90 min after the injection of lidocaine. **E-E4**, spinalization removes the post-lidocaine increase in correlation. **F-F4**, after a second injection of lidocaine the segmental distribution of the coefficients of correlation resembles the configuration attained 10-20 min after the first administration of lidocaine. The coefficients of similarity (RMSS) between correlograms generated under different experimental conditions are indicated by the brackets. Red numbers denote correlograms with highest similarity. Same experiment as that of Fig. 1. Further explanations in text.

Figure 3.- Differential effects of capsaicin and lidocaine on the correlation of superficial and deep intraspinal fields with the CDPs recorded from different segments. The graphs with the horizontal bars display the coefficients of correlation arranged in descending order. The segmental distribution of these coefficients is shown in the right. In both graphs the colors indicate the magnitude of the correlation (see scale). Separate plots were made for the correlations of the S-IFPs and D-IFPs with the CDPs as indicated. Location of intraspinal electrodes is shown in Fig. 1. The brackets show the RMSS values between different pairs of correlograms. Numbers in red indicate denote the lowest RMSS values, suggesting similar distributions. Same experiment as that of Fig.1 and 2. See text for further explanations.

Figure 4.- The differential effects of capsaicin on the functional connectivity between dorsal horn neurones are transiently reversed by lidocaine and suppressed by spinalization. Panels **A-I** show the graphs obtained by plotting the control coefficients of correlation between paired sets of CDPs (Control 0, abscissae) versus the coefficients obtained at different times before and during the action of capsaicin (**A-C**), after lidocaine (**D-G**), after spinalization (**H**) and after a second administration of lidocaine (**I**). Note that after capsaicin the coefficients of correlation were separated in two distinct clusters that persisted without substantial

changes until the injection of lidocaine transiently reverted the effects of capsaicin giving rise to a single cluster. After spinalization the post-lidocaine two-cluster arrangement of the coefficients changed to a single cluster. The RMSS similarity coefficients between the different correlograms as well as the ANCOVA p values for the C1 and C2 components are included in the figure. **J-R,** effects of capsaicin, lidocaine and spinalization on the correlation of the S-IFPS and D-IFPs with the CDPs. Data obtained from the same experiment as that of Fig. 1-3. See text for further details.

Figure 5.- Consistency of effects on correlation between CDPs produced by capsaicin and lidocaine in preparations with intact neuraxis. A, B and C, data from 3 different experiments showing correlograms and graphs relating control coefficients of correlation versus effects produced by capsaicin and lidocaine as indicated. Note that despite the differences in the control correlograms in the three experiments, capsaicin increased the correlation between CDPs and lidocaine transiently reversed the effects of capsaicin. RSMM coefficients of similarity between different correlograms are indicated in the figure. Bars at the bottom show timing of the different procedures. See text for further details.

Figure 6.- Systemic lidocaine transiently reverses the capsaicin-induced increase in power spectra and coherence between CDPs. A-C, power spectra of the CDPs recorded from segments L6cL (black traces) and L6cR (blue traces) before, 10-20 min and 80-90 min after the intradermic injection of capsaicin. **D**, **E** power spectra obtained from recordings made 10-20 min and 80-90 min after the systemic administration of lidocaine. **F,** 10-20 min after spinalization. **G**, second dose of lidocaine injected 60-70 min after spinalization. **H-L,** superposed traces of the normalized spectra of the L6cL CDPs allow comparison of the changes in the different frequency components produced by capsaicin, lidocaine and spinalization, as indicated (see colors). **M-S**, segmental distribution of the changes in power spectra produced by capsaicin, lidocaine and spinalization. Graphs show

frequency of power spectra versus segmental location of the recording sites. Frequency changes in left (L) and right (R) sides are plotted separately as mirror images (see abscissa). The colors indicate the magnitude of the power spectra in logarithmic scale (see calibration). Note the expansion of the capsaicin-induced spectral increase towards the more rostral segments and the transient suppression of this effect by lidocaine. **T-W**, changes in coherence between CDPs produced by the different experimental procedures in four frequency ranges as indicated (see red arrows and gray bars in control spectra displayed in A). Note that the capsaicin increase in coherence is largest in the low frequency range (1.5-4.5Hz). Same experiment as that of Figs.1 and 2. Further explanations in text.

Figure 7.- Supraspinal dependence of the effects of capsaicin and lidocaine on the correlation between ongoing CDPs and IFPs. Same format as that of Figure 1. **A-E**, raw recordings of the CDPs and IFPs obtained after spinalization, capsaicin and lidocaine, as indicated. **F**, vertical display of the coefficients of correlation obtained from sets of 5 min continuous recordings displayed taking as reference the distribution of the Control 0 coefficients. **G-H, c**orrelation of S-IFPs and D-IFPs with CDPs. Insert shows spinal location of IFP recording sites. See text for further explanations.

Figure 8.- The effects of capsaicin and lidocaine on the segmental distribution of the correlation between the CDPs are subjected to a supraspinal control. A-E, same format as that of Fig. 2. The effects of the different procedures are indicated in each panel. Note that after spinalization the segmental distribution of the coefficients of correlation was not significantly changed by capsaicin and lidocaine. The RMSS values between different correlograms are indicated. **F-J** graphs obtained by plotting the control coefficients of correlation between CDPs (Control 0, abscissae) versus the coefficients obtained at different times as indicated. Ps was >0.05 for both C1 and C2 in Spinal

10-15 min vs Cap 65-70 min, Cap 65-70 min vs Lido 15-20 min and Lido 15-20 min vs Lido 55-60 min. See text for further explanations.

Figure 9.- Changes in correlation produced by capsaicin and lidocaine in previously spinalized preparations. A and B data from 2 different experiments showing correlograms and graphs relating control coefficients of correlation versus changes induced by different procedures as indicated. Same format as that of Fig. 5. Note that after spinalization, capsaicin and lidocaine had rather small effects on the correlation between CDPs. RMSS values between different correlograms, best linear fits and Ps values are indicated in the figures. Bars at the bottom show timing of the different procedures. See text for further details.

Figure 10.- Spinalization greatly attenuates the effects of capsaicin and lidocaine on the power spectra and coherence between CDPs seen in preparations with intact neuroaxis. Same format as that of Fig. 6. **A-F**, changes in the power spectra of CDPs recorded from segments L6rL (black traces) and L6rR (blue traces) during several experimental procedures, as indicated. **G-L**, graphs showing frequency versus segmental location of the changes in power spectra produced by spinalization, capsaicin and lidocaine. Note that after spinalization, capsaicin slightly increases the power spectra in the low frequency range and that this effect was mildly reduced by lidocaine, particularly in the right side. Recordings of L7rR were not available. **M-P**, changes in coherence between CDPs produced by the different experimental procedures in four frequency ranges as indicated. Note that lidocaine has a rather weak action on the capsaicin changes induced after spinalization, particularly for frequencies above 9.5 Hz. Further explanations in text.

Figure 11.- Systemic lidocaine transiently reverses the facilitation of the spinal responses evoked by mechanical stimulation in the region of secondary hyperalgesia as well as the capsaicin-induced disruption of correlation between CDPs. A, CDPs produced by mechanical stimulation of the

skin with an air puff applied close to the site of capsaicin injection (Site 1). **B**, same as A, following mechanical stimulation farther away from the capsaicin-injection site (35 mm), within the region of secondary hyperalgesia (Site 2). The numbers indicate percentage changes in peak amplitude of the mechanically evoked responses relative to the amplitude of the control responses. **C-F** changes in the coefficients of correlation between paired sets of CDPs produced by capsaicin and lidocaine at the indicated times. Numbers show the RMSS values between pairs of correlograms obtained at different times after capsaicin and lidocaine, as indicated. **G-J**, plots of the control 0 coefficients (abscissae) against the correlation coefficients obtained under the different experimental procedures (ordinates). The graphs **H** and **J** show that the separation between the two clusters observed 60-70 min after capsaicin was transiently reduced 30-40 min after lidocaine. At that time the correlogram resembled the control one (RMSS value 0.34). 50-60 min after lidocaine the coefficients were again distributed in two similar clusters resembling those displayed 60-70 min after capsaicin (Ps> 0.05 for both C1 and C2). Bar at the bottom shows timing of the different procedures. See text for further details.

Fig. 12.- After acute spinalization the effects of capsaicin and lidocaine on the responses produced by mechanical stimulation of the skin as well as on the correlation between CDPs are strongly attenuated. Same format as Fig. 11. **A**, Effects of spinalization, capsaicin and lidocaine on the CDPs recorded in the rostral and caudal regions of the L5 and L6 segments following tactile stimulation of the skin close to the site of capsaicin injection (Site 1, primary hyperalgesia). **B**, effects on CDPs evoked by mechanical stimulation away from the capsaicin-injection site (35 mm), within the region of secondary hyperalgesia (Site 2). The numbers indicate percentage changes in peak amplitude of the mechanically evoked responses relative to the amplitude of the responses produced after spinalization. **C-G** changes in the coefficients of correlation between CDPs produced by capsaicin and lidocaine at the indicated times. RMSS values between correlograms are shown. **H-L**, plots of the control 0 coefficients (abscissae) against

the correlation coefficients obtained under different experimental procedures (ordinates). Note that spinalization separated the coefficients in two clusters. Capsaicin slightly reduced the correlation between the paired sets of CDPs grouped in cluster C2, practically without affecting the correlation between CDPs in cluster C1. Lines show best linear fits. Ps ><0.05 for C12 and C2 and Ps>0.05 for C1 in Spinal 30-35 min vs Cap 70-75 min, . Ps >0.05 for C1 and C2 in Cap 70-75 min vs Lido 15-20 min and Lido 15-20 min vs Lido 40-45 min. Bar at the bottom shows timing of the different procedures. See text for further explanations.

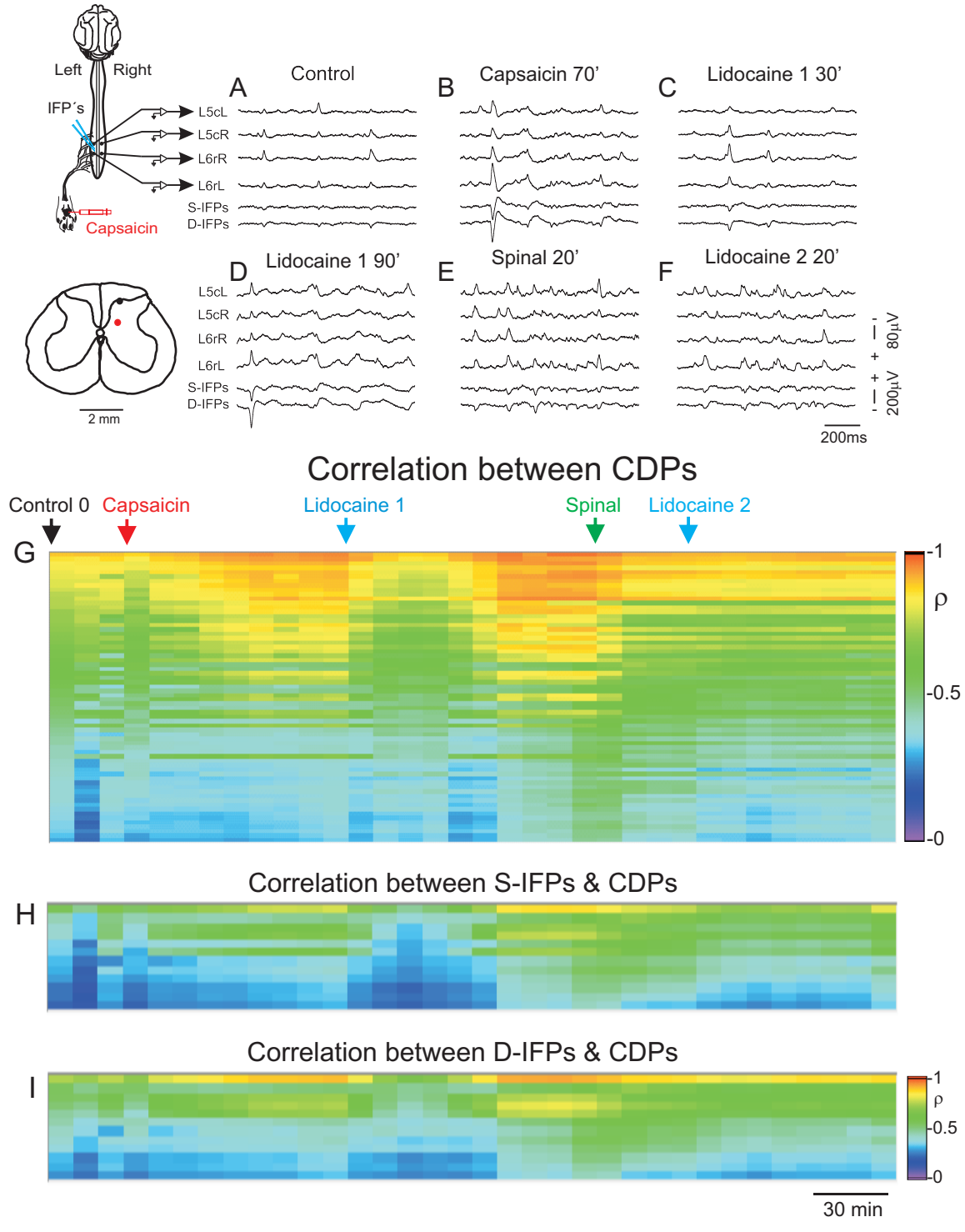
Left
Right
IFP´s
L5cL
L5cR
L6rR
L6rL
S-IFPs
D-IFPs
Capsaicin
A
Control
B
Capsaicin 70'
C
Lidocaine 1 30'
D
Lidocaine 1 90'
E
Spinal 20'
F
Lidocaine 2 20'
2 mm
80µV
200µV
200ms
Correlation between CDPs
Control 0
Capsaicin
Lidocaine 1
Spinal
Lidocaine 2
G
-1
ρ
-0.5
-0
Correlation between S-IFPs & CDPs
H
Correlation between D-IFPs & CDPs
I
30 min

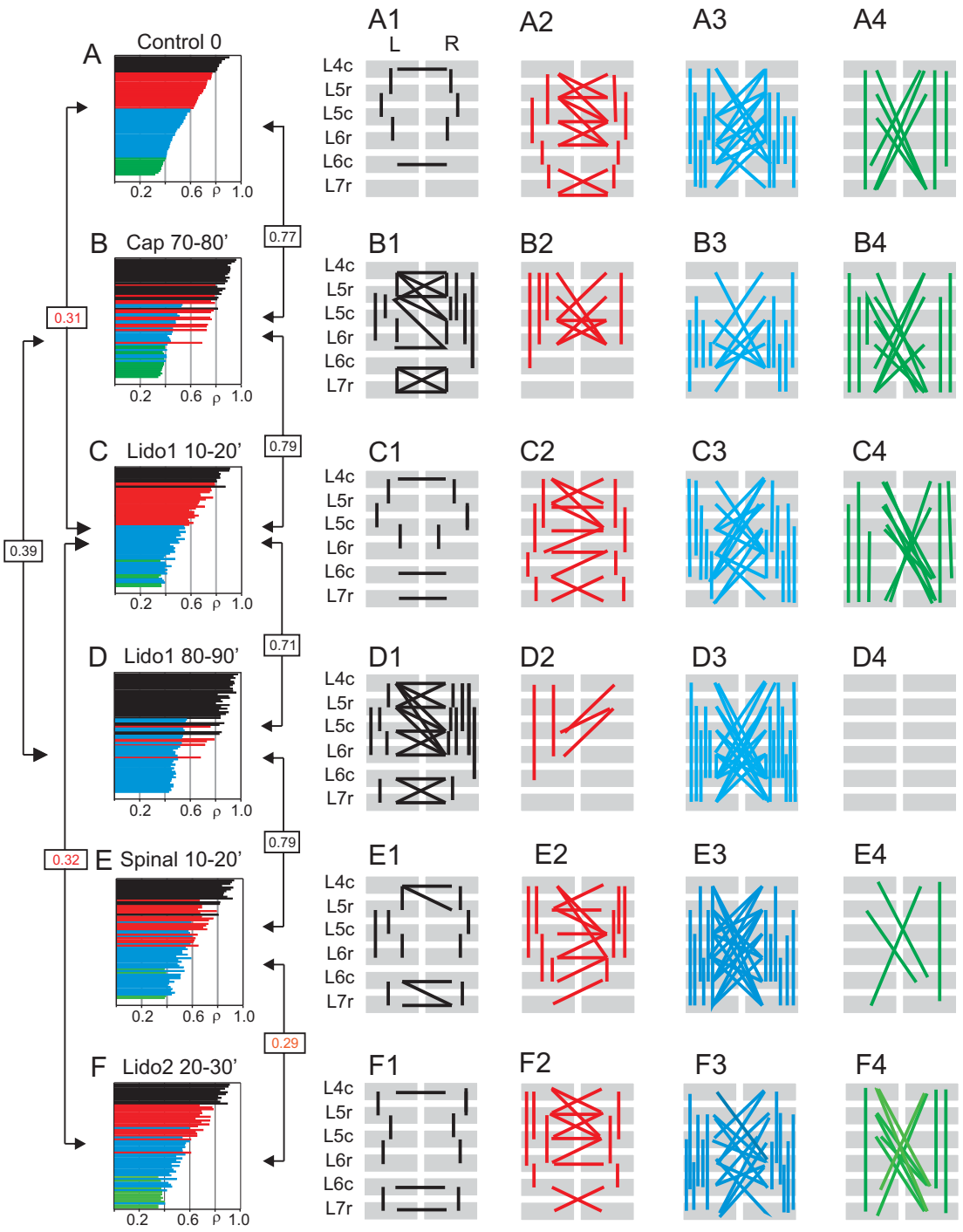
A
Control 0
B
Cap 70-80'
C
Lido1 10-20'
D
Lido1 80-90'
E
Spinal 10-20'
F
Lido2 20-30'
0.2
0.6
ρ
1.0
0.77
0.31
0.79
0.39
0.71
0.79
0.32
0.29
A1
L
R
A2
A3
A4
B1
B2
B3
B4
C1
C2
C3
C4
D1
D2
D3
D4
E1
E2
E3
E4
F1
F2
F3
F4
L4c
L5r
L5c
L6r
L6c
L7r

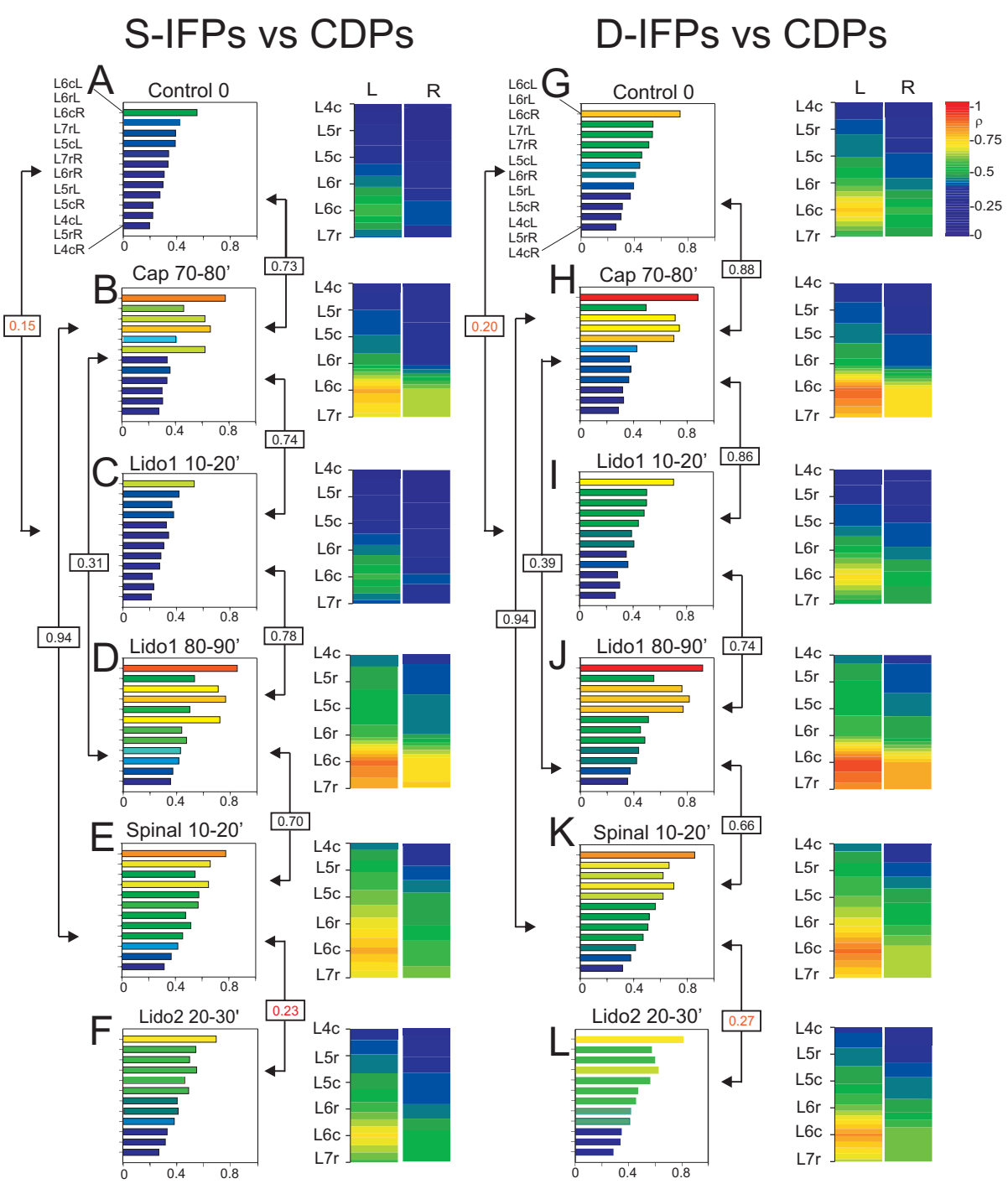
S-IFPs vs CDPs
D-IFPs vs CDPs
A
Control 0
B
Cap 70-80'
C
Lido1 10-20'
D
Lido1 80-90'
E
Spinal 10-20'
F
Lido2 20-30'
G
Control 0
H
Cap 70-80'
I
Lido1 10-20'
J
Lido1 80-90'
K
Spinal 10-20'
L
Lido2 20-30'
L6cL
L6rL
L6cR
L7rL
L5cL
L7rR
L6rR
L5rL
L5cR
L4cL
L5rR
L4cR
L4c
L5r
L5c
L6r
L6c
L7r
L
R
0
0.4
0.8
ρ
1
0.75
0.5
0.25
0
0.15
0.73
0.74
0.31
0.94
0.78
0.70
0.23
0.20
0.88
0.86
0.39
0.94
0.74
0.66
0.27

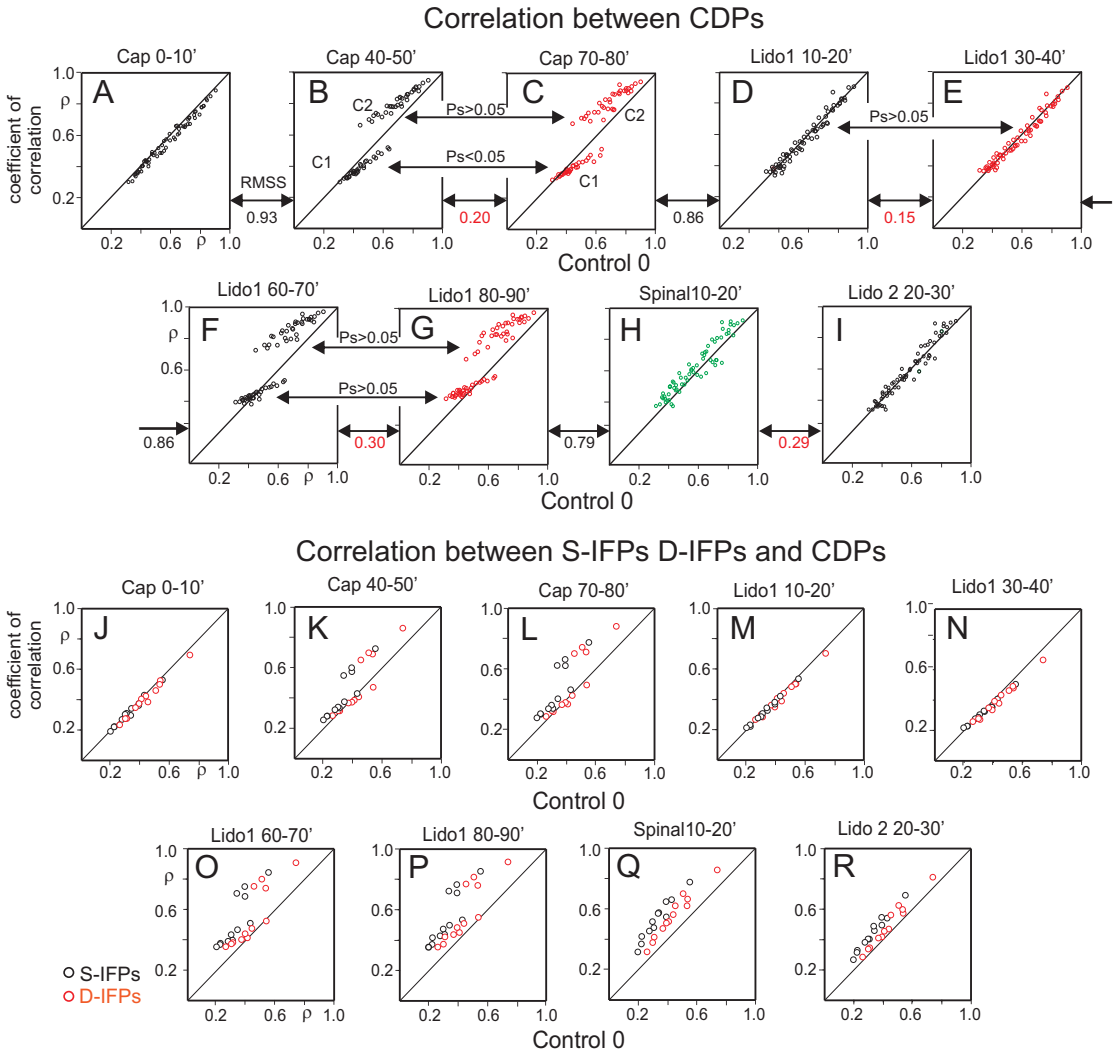
Correlation between CDPs
Cap 0-10'
Cap 40-50'
Cap 70-80'
Lido1 10-20'
Lido1 30-40'
coefficient of correlation
A
B
C
D
E
RMSS
0.93
C2
C1
Ps>0.05
Ps<0.05
0.20
0.86
0.15
Control 0
Lido1 60-70'
Lido1 80-90'
Spinal10-20'
Lido 2 20-30'
F
G
H
I
0.86
0.30
0.79
0.29
Control 0
Correlation between S-IFPs D-IFPs and CDPs
J
K
L
M
N
Control 0
O
P
Q
R
S-IFPs
D-IFPs
Control 0

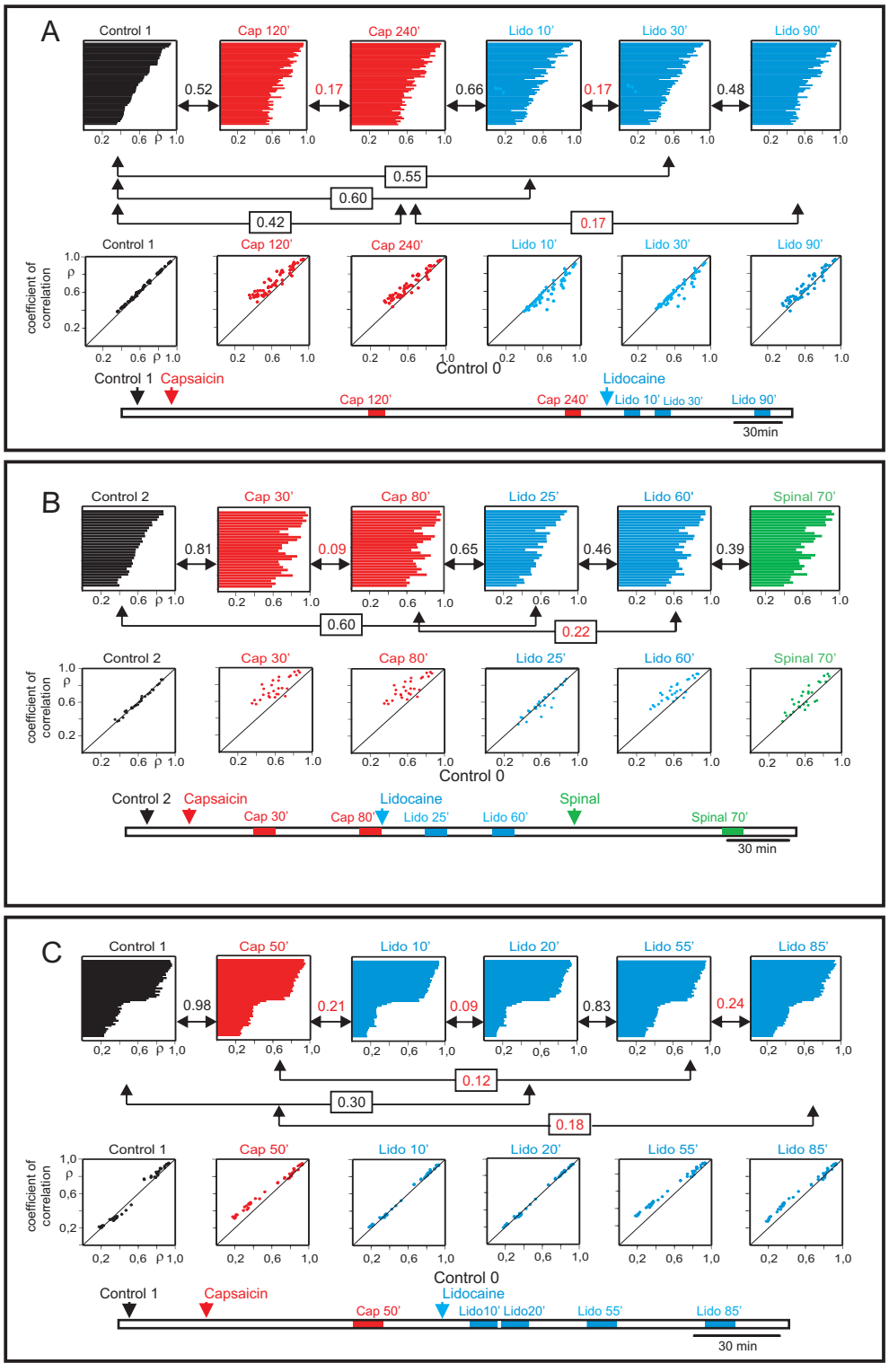
A
Control 1
Cap 120'
Cap 240'
Lido 10'
Lido 30'
Lido 90'
0.52
0.17
0.66
0.17
0.48
0.55
0.60
0.42
0.17
coefficient of correlation
Control 0
Control 1
Capsaicin
Lidocaine
30min
B
Control 2
Cap 30'
Cap 80'
Lido 25'
Lido 60'
Spinal 70'
0.81
0.09
0.65
0.46
0.39
0.60
0.22
Control 0
Control 2
Capsaicin
Lidocaine
Spinal
30 min
C
Control 1
Cap 50'
Lido 10'
Lido 20'
Lido 55'
Lido 85'
0.98
0.21
0.09
0.83
0.24
0.12
0.30
0.18
Control 0
Control 1
Capsaicin
Lidocaine
30 min

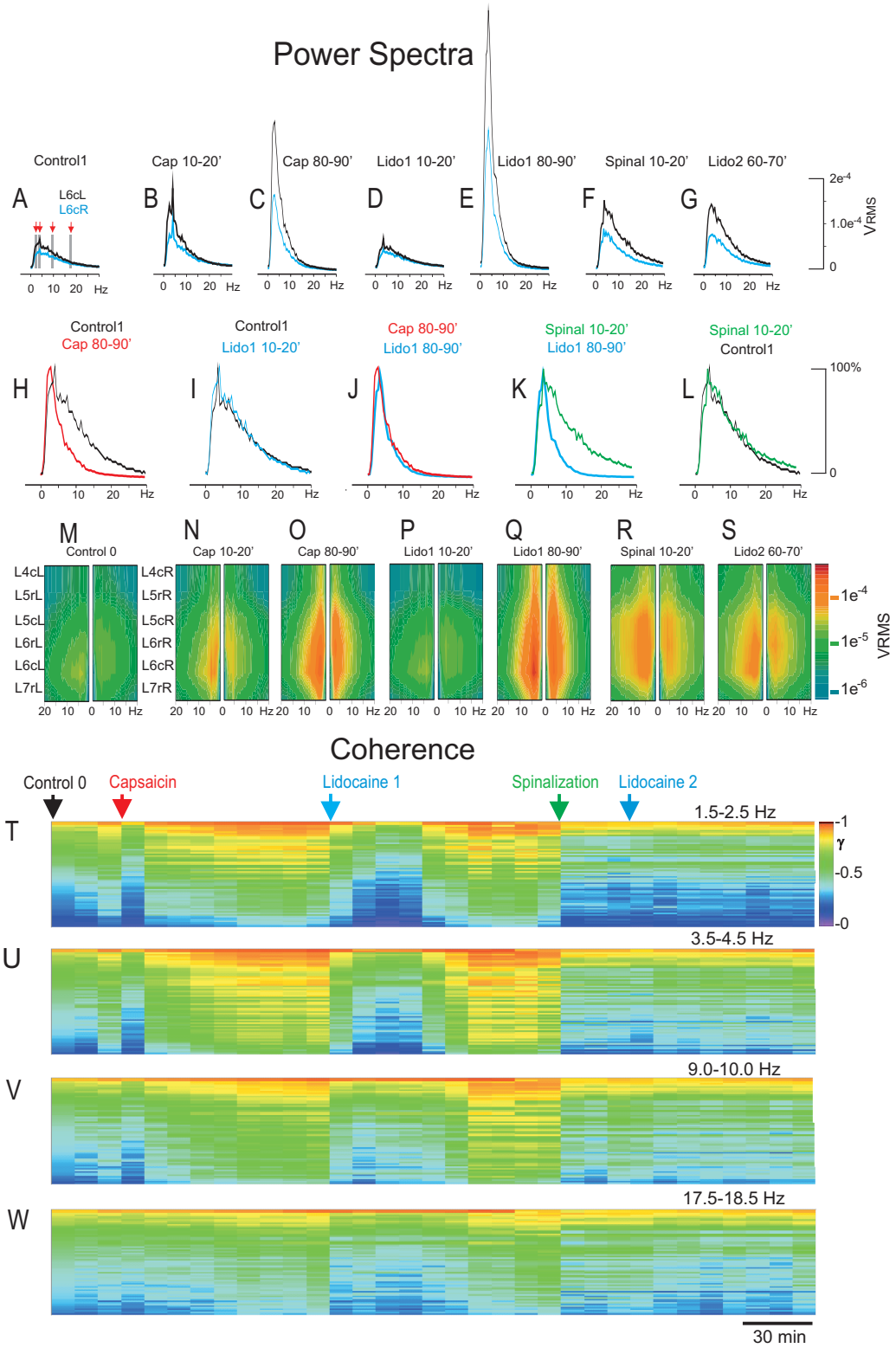
Power Spectra
Control1
Cap 10-20'
Cap 80-90'
Lido1 10-20'
Lido1 80-90'
Spinal 10-20'
Lido2 60-70'
A
L6cL
L6cR
B
C
D
E
F
G
0 10 20 Hz
2e-4
1.0e-4
0
VRMS
Control1
Cap 80-90'
Control1
Lido1 10-20'
Cap 80-90'
Lido1 80-90'
Spinal 10-20'
Lido1 80-90'
Spinal 10-20'
Control1
H
I
J
K
L
100%
0
M
Control 0
N
Cap 10-20'
O
Cap 80-90'
P
Lido1 10-20'
Q
Lido1 80-90'
R
Spinal 10-20'
S
Lido2 60-70'
L4cL
L5rL
L5cL
L6rL
L6cL
L7rL
L4cR
L5rR
L5cR
L6rR
L6cR
L7rR
20 10 0 10 Hz
1e-4
1e-5
1e-6
VRMS
Coherence
Control 0
Capsaicin
Lidocaine 1
Spinalization
Lidocaine 2
T
1.5-2.5 Hz
-1
γ
-0.5
-0
U
3.5-4.5 Hz
V
9.0-10.0 Hz
W
17.5-18.5 Hz
30 min

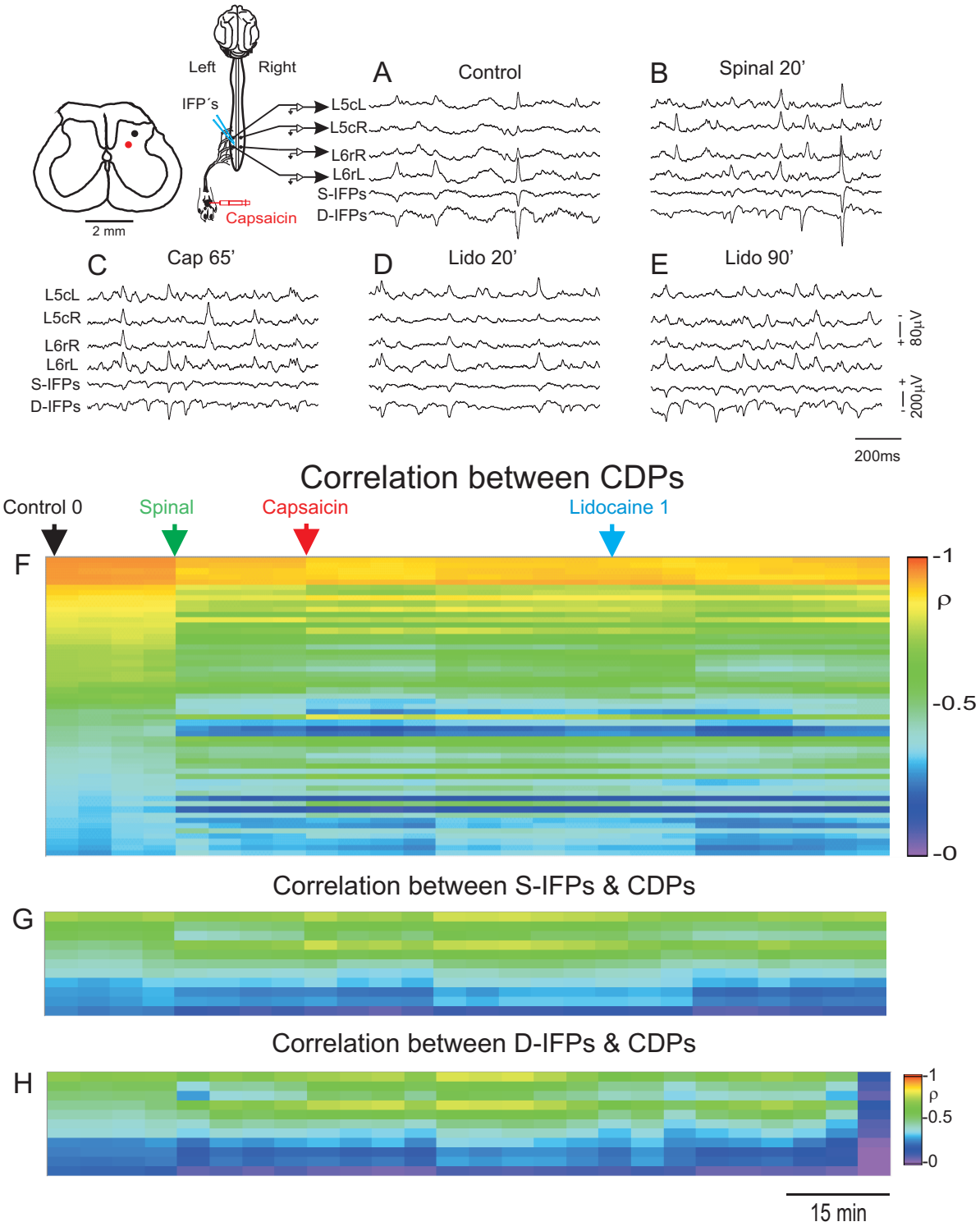
Left
Right
IFP´s
Capsaicin
2 mm
A
Control
L5cL
L5cR
L6rR
L6rL
S-IFPs
D-IFPs
B
Spinal 20'
C
Cap 65'
D
Lido 20'
E
Lido 90'
80µV
200µV
200ms
Correlation between CDPs
Control 0
Spinal
Capsaicin
Lidocaine 1
F
-1
ρ
-0.5
-0
Correlation between S-IFPs & CDPs
G
Correlation between D-IFPs & CDPs
H
15 min

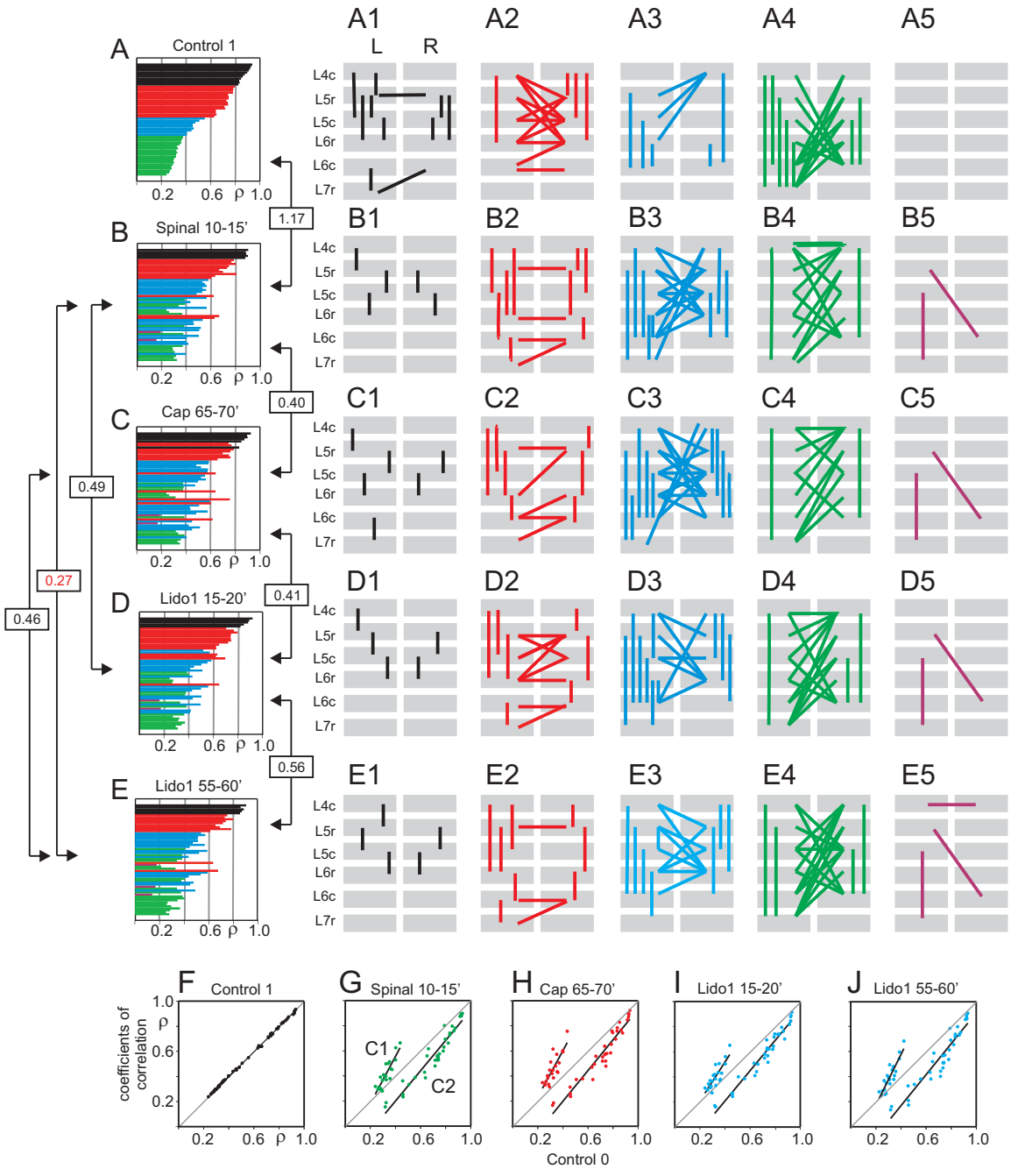
A
Control 1
B
Spinal 10-15'
C
Cap 65-70'
D
Lido1 15-20'
E
Lido1 55-60'
0.2 0.6 ρ 1.0
1.17
0.40
0.41
0.56
0.49
0.27
0.46
A1 A2 A3 A4 A5
B1 B2 B3 B4 B5
C1 C2 C3 C4 C5
D1 D2 D3 D4 D5
E1 E2 E3 E4 E5
L R
L4c
L5r
L5c
L6r
L6c
L7r
F Control 1
G Spinal 10-15'
H Cap 65-70'
I Lido1 15-20'
J Lido1 55-60'
coefficients of correlation
ρ
1.0
0.6
0.2
C1
C2
Control 0

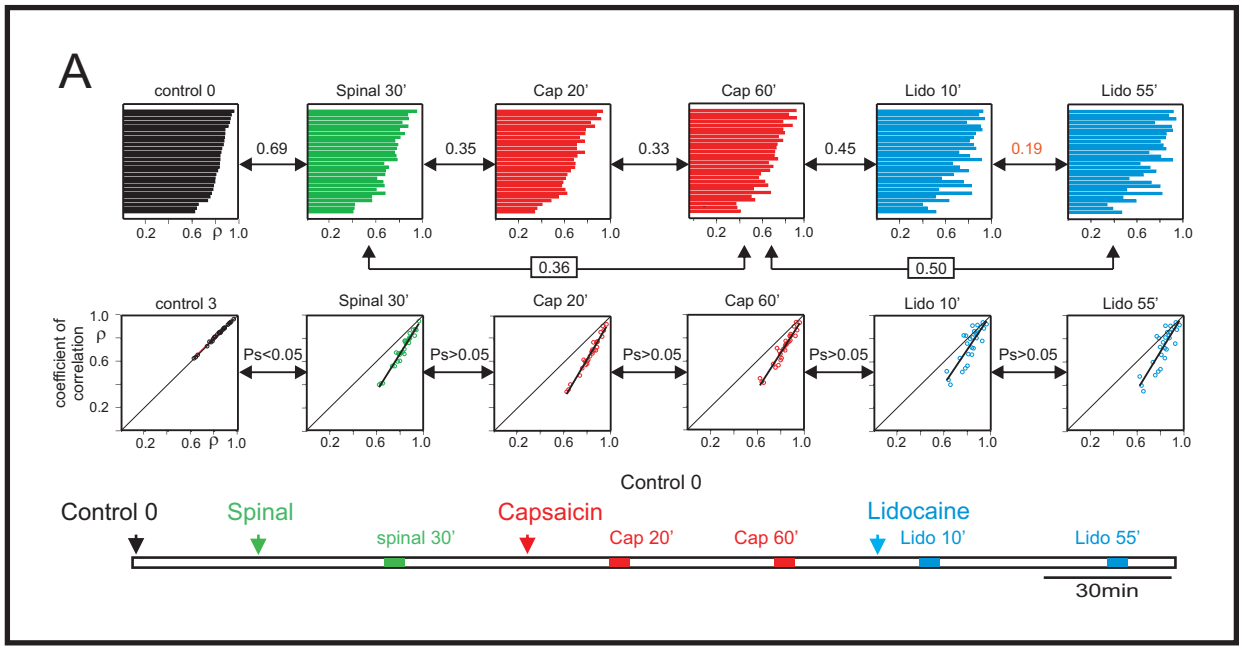
A
control 0
Spinal 30'
Cap 20'
Cap 60'
Lido 10'
Lido 55'
0.69
0.35
0.33
0.45
0.19
0.36
0.50
control 3
coefficient of correlation
Ps<0.05
Ps>0.05
Control 0
Control 0
Spinal
Capsaicin
Lidocaine
spinal 30'
Cap 20'
Cap 60'
Lido 10'
Lido 55'
30min

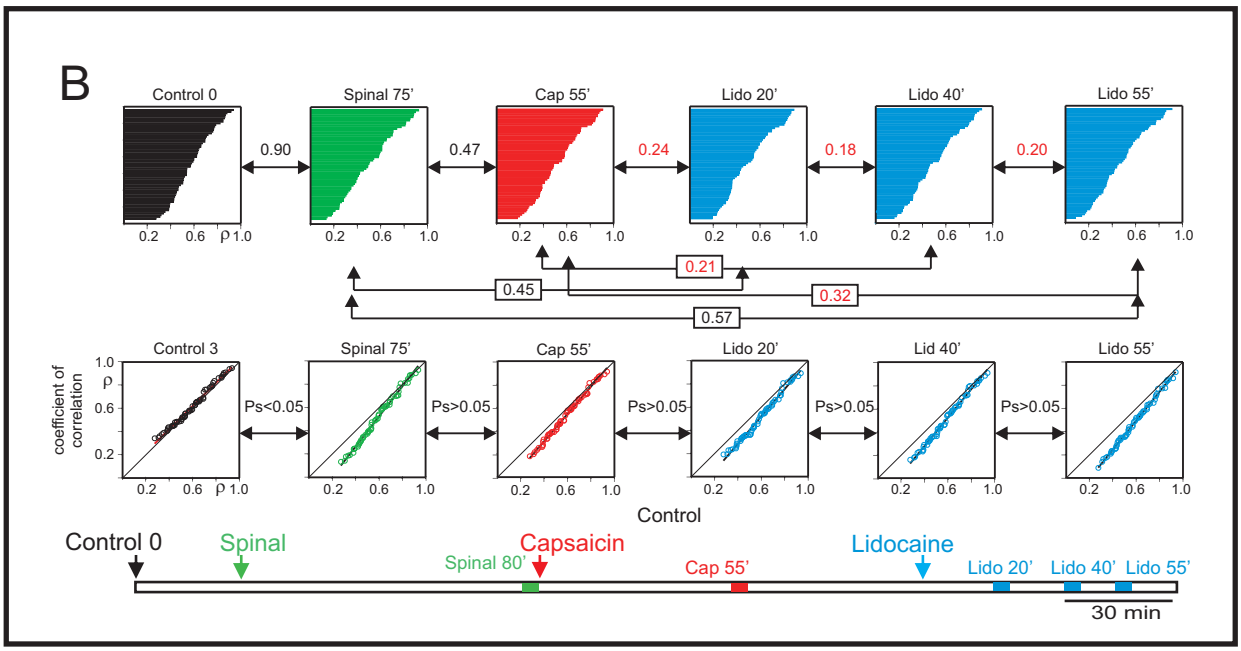
B
Control 0
Spinal 75'
Cap 55'
Lido 20'
Lido 40'
Lido 55'
0.90
0.47
0.24
0.18
0.20
0.21
0.45
0.32
0.57
Control 3
Lid 40'
coefficient of correlation
Ps<0.05
Ps>0.05
Control
Control 0
Spinal
Capsaicin
Lidocaine
Spinal 80'
Cap 55'
Lido 20'
Lido 40'
Lido 55'
30 min

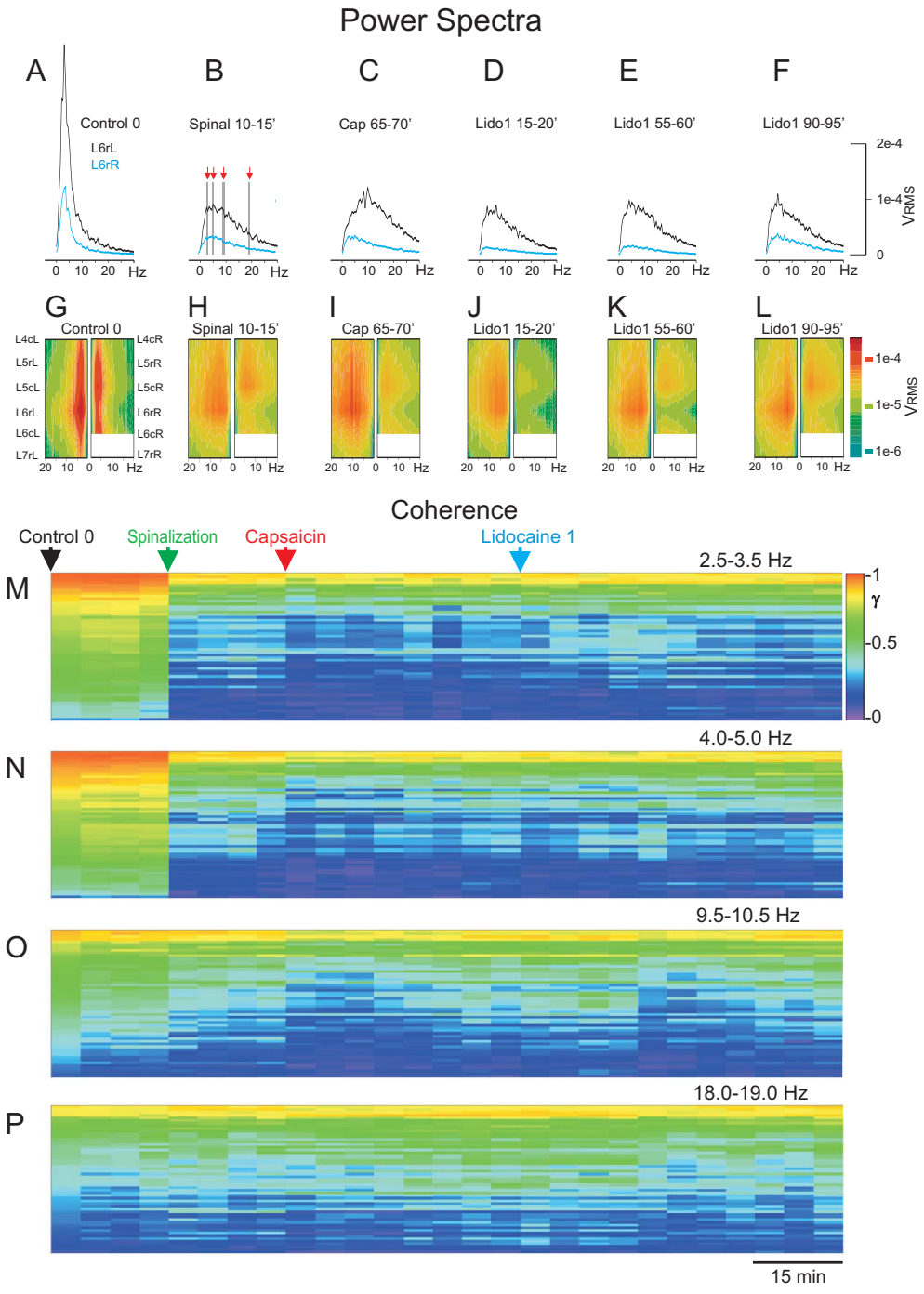
Power Spectra
A
B
C
D
E
F
Control 0
Spinal 10-15'
Cap 65-70'
Lido1 15-20'
Lido1 55-60'
Lido1 90-95'
L6rL
L6rR
0 10 20 Hz
2e-4
1e-4
0
VRMS
G
H
I
J
K
L
L4cL
L5rL
L5cL
L6rL
L6cL
L7rL
L4cR
L5rR
L5cR
L6rR
L6cR
L7rR
20 10 0 10 Hz
1e-4
1e-5
1e-6
Coherence
Control 0
Spinalization
Capsaicin
Lidocaine 1
M
2.5-3.5 Hz
γ
-1
-0.5
-0
N
4.0-5.0 Hz
O
9.5-10.5 Hz
P
18.0-19.0 Hz
15 min

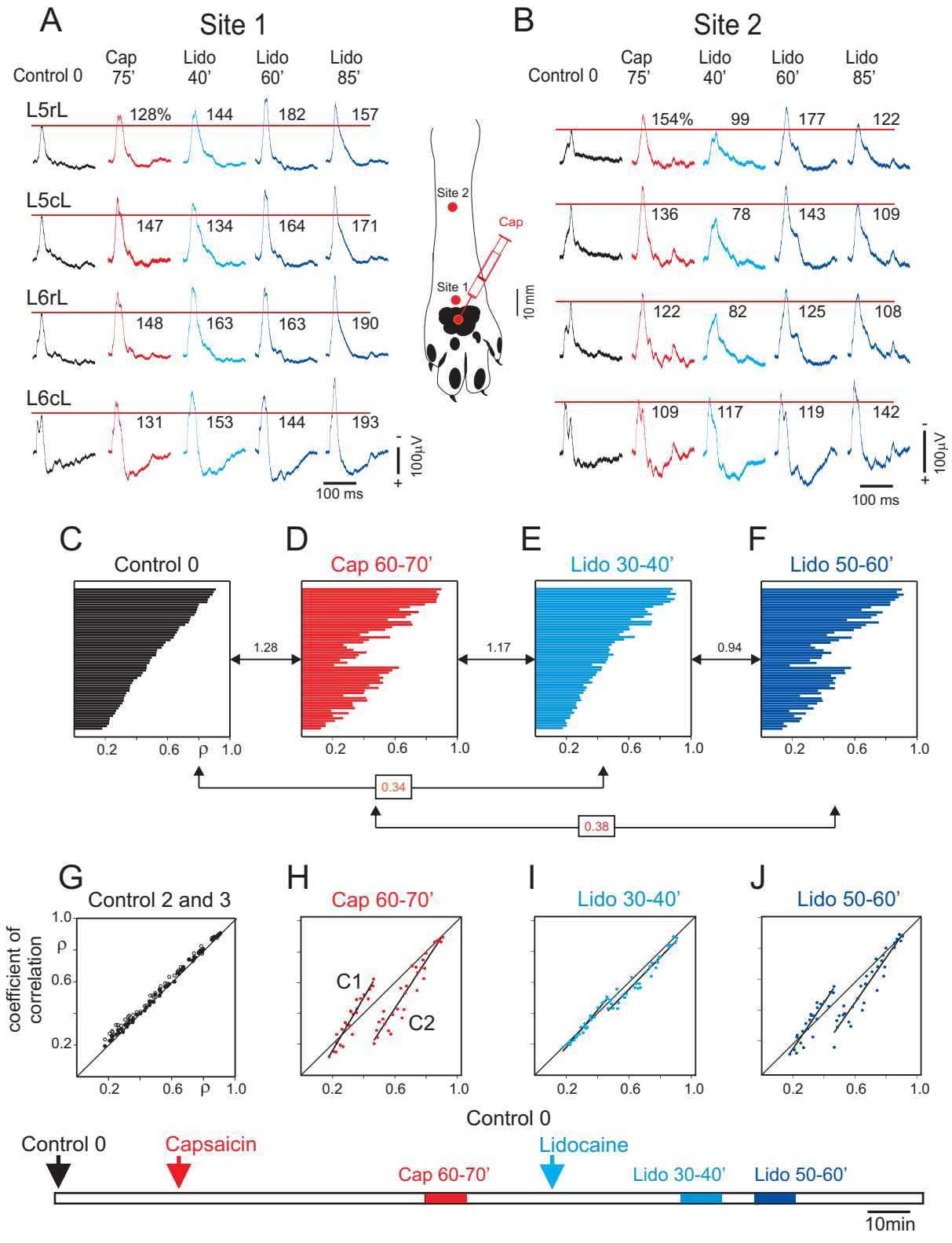
A
Site 1
Control 0
Cap 75'
Lido 40'
Lido 60'
Lido 85'
L5rL
128%
144
182
157
L5cL
147
134
164
171
L6rL
148
163
163
190
L6cL
131
153
144
193
100 ms
100µV
Site 2
Cap
Site 1
10 mm
B
Site 2
Control 0
Cap 75'
Lido 40'
Lido 60'
Lido 85'
154%
99
177
122
136
78
143
109
122
82
125
108
109
117
119
142
100 ms
100µV
C
Control 0
D
Cap 60-70'
E
Lido 30-40'
F
Lido 50-60'
1.28
1.17
0.94
0.2
0.6
ρ
1.0
0.34
0.38
G
Control 2 and 3
H
Cap 60-70'
I
Lido 30-40'
J
Lido 50-60'
coefficient of correlation
1.0
ρ
0.6
0.2
C1
C2
Control 0
Control 0
Capsaicin
Lidocaine
Cap 60-70'
Lido 30-40'
Lido 50-60'
10min

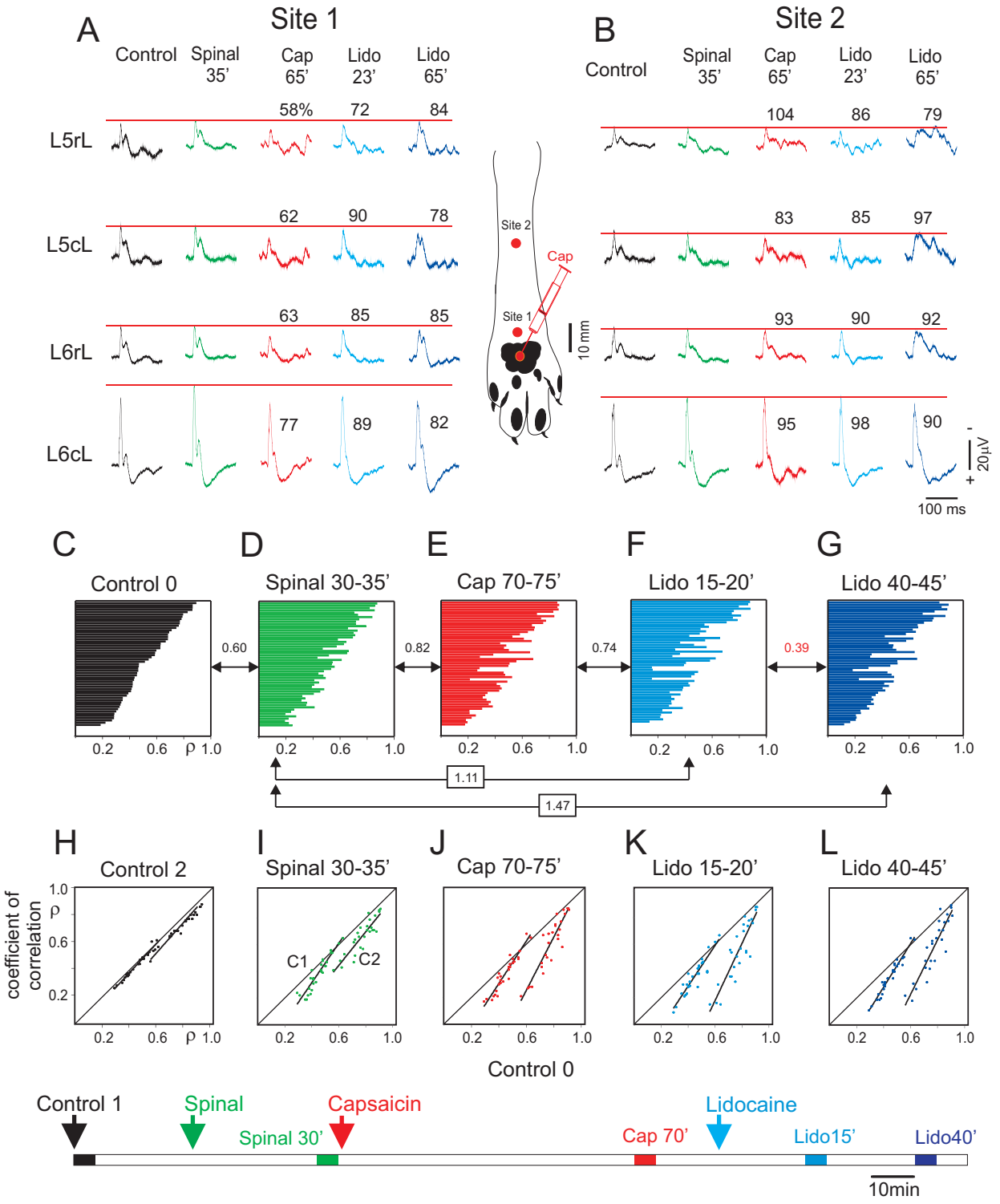
A
Site 1
Control
Spinal 35'
Cap 65'
Lido 23'
Lido 65'
L5rL
58%
72
84
L5cL
62
90
78
L6rL
63
85
85
L6cL
77
89
82
Site 2
Cap
Site 1
10 mm
B
Site 2
Control
Spinal 35'
Cap 65'
Lido 23'
Lido 65'
104
86
79
83
85
97
93
90
92
95
98
90
20µV
100 ms
C
Control 0
D
Spinal 30-35'
E
Cap 70-75'
F
Lido 15-20'
G
Lido 40-45'
0.60
0.82
0.74
0.39
0.2
0.6
ρ 1.0
1.11
1.47
H
Control 2
I
Spinal 30-35'
J
Cap 70-75'
K
Lido 15-20'
L
Lido 40-45'
coefficient of correlation
1.0
ρ
0.6
0.2
C1
C2
Control 0
Control 1
Spinal
Capsaicin
Spinal 30'
Cap 70'
Lidocaine
Lido15'
Lido40'
10min